Dye-Sensitized Solar Hydrogen Production: the Emerging Role of Metal-Free Organic Sensitizers

Bianca Cecconi,[a] Norberto Manfredi,[a] Tiziano Montini,[b] Paolo Fornasiero,[b] and Alessandro Abbotto*[a]

Abstract: The production of hydrogen from sunlight and water is gaining an increasingly important role in the production of clean fuels from sustainable and abundant energy sources. In this process, commonly referred to as artificial photosynthesis, the role of the dye-sensitizer is critical for optimizing the harvesting of visible light and triggering the reduction reaction at the catalytic active site. In recent decades organometallic sensitizers have been mainly studied, often implying the use of scarce and, in some cases, toxic elements. This microreview describes the state of the art in the use of metal-free organic sensitizers, highlighting advantages compared to their organometallic counterparts. Main design and synthetic strategies, specific properties, and device performances are presented. Thanks to recent advances and lower manufacturing costs, organic sensitizers will gain increasing importance for next generation clean fuels.

1. Introduction

Future energy needs will increasingly benefit from renewable sources such as sunlight.[1] Accordingly, in the last years many scientists have focused their research efforts in investigating new materials to efficiently convert the solar radiation to electric current in last generation photovoltaic (PV) devices.[2],[3] However, electricity accounts for only a minor portion of total energy needs, being more than 60% of the present world energy consumption constituted by fuels for transportation and synthesis of chemical intermediates.[4] In particular, in the field of transportation, important recent technological progresses have been made for electrical-powered vehicles but still not sufficient to replace present fossil fuel combustion engines.[5] Meanwhile, in the long-term roadmap to progressively shift to an electricity-based economy over the course of the 21st century, fuels will play a prominent role for many decades. Therefore, it is critically important to develop new technologies to access the production of fuels in a renewable and clean manner to phase out fossil sources.

[a] Dr. B. Cecconi, Dr. N. Manfredi, and Prof. A. Abbotto
Department of Materials Science, Solar Energy Research Center
MIB-SOLAR and INSTM Milano-Bicocca Research Unit
University of Milano-Bicocca, Via Cozzi 55, I-20125, Milano, Italy
E-mail: alessandro.abbotto@unimib.it
Homepage URL: http://www.stc.unimib.it/abbotto/

[b] Dr. T. Montini, and Prof. P. Fornasiero
Department of Chemical and Pharmaceutical Sciences; ICCOM-CNR Trieste Research Unit and INSTM Trieste Research Unit
University of Trieste, Via L.Giorgieri 1, I-34127 Trieste, Italy

Hydrogen is an ideal energy carrier since it has no carbon footprint and can be obtained from an inexhaustible and sustainable source as water.[6] Hydrogen can be used as a fuel in fuel cells to cleanly produce electricity and power electrical vehicles beyond the limits of battery-powered cars. Finally, it can be used as main reagent to produce synthetic fuels or industrially important chemical intermediates starting from carbon sources (e.g, CO_2 reduction to CH_4, CH_3OH, etc.).[7]
Nature gives a hint through the natural photosynthetic process that is, very schematically, the dye-sensitized solar-induced splitting of water to yield oxygen and “reduction equivalents” of hydrogen, which are then exploited to reduce carbon dioxide and generate carbohydrates. Similarly, scientists can mimic this process and fabricate an artificial photosynthetic process to produce solar fuels starting from water and sunlight.[8]
The standard potential $\Delta E°$ of water splitting or water electrolysis to H_2 and O_2 (Equation 1) is 1.23 V at any pH (Equation 1).

$$H_2O \longrightarrow H_2 + 1/2\ O_2 \quad (1)$$

From the reaction stoichiometry, the volume of produced hydrogen is twice that of oxygen. In energetic terms, water splitting requires a free energy $\Delta G° = -nF\ \Delta E°$ (where F is the Faraday constant, 96485.3365 C mol^{-1}). For the splitting of 1 mol of H_2O to 1 mol of H_2 and 0.5 mol of O_2, n is equal to 2 electrons and $\Delta G° = -2 \times 96485$ C $mol^{-1} \times -1.23$ J $C^{-1} = 237$ kJ mol^{-1} H_2O or $\Delta G° = 2.46$ eV mol^{-1} H_2O (with 1 eV = 96.48 kJ mol^{-1}). Accordingly, for each electron involved in the redox reaction, the free energy is 1.23 eV. Water splitting is a multi-electronic (2 electrons per each molecule of hydrogen and 4 electrons per each molecule of oxygen evolved), multi-atomic thermodynamic energy demanding, and kinetically hampered process with a high activation barrier (Figure 1).

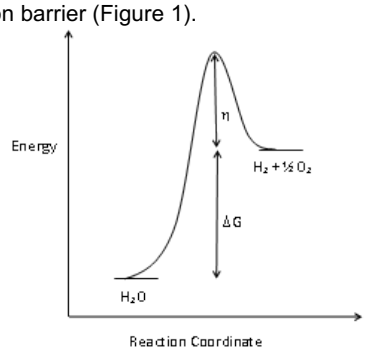

Figure 1: Energetic path of water splitting process.

Thermodynamic losses and overpotentials associated to the reaction kinetics increase the voltage required for water splitting

to higher values, up to 1.8 - 2.0 V, the typical voltage at which commercial electrolyzers operate.[9]

Two main methods can be used to perform water splitting from solar energy: 1) PV-driven electrolysis, that is electrolysis of water using a solar cell in combination with an electrolyzer; 2) integrated system: photocatalytic system or a photoelectrochemical cell (PEC).[10] A further method exploiting solar energy implies reforming of biomasses.[9-11] The use of PV electric energy to run electrolysis of water is a relatively efficient way to produce hydrogen, but the cost estimation (~ 2.6 €/Kg of hydrogen) of the whole process is too high to ever compete with steam reforming of methane (~ 1 €/kg of hydrogen).[10a] Therefore the second approach, either via PEC or photocatalysis, is the only one potentially capable to sustainably produce hydrogen at competitive costs. Unfortunately, solar-to-hydrogen efficiencies are still very low.[10a] This approach has been pioneered in 1972 by the remarkable work by Honda and Fujishima, who first introduced TiO_2 in combination with Pt nanoparticles to run water splitting in a PEC device. The Honda-Fujishima experiment laid the bases for the future development of artificial photosynthesis, but the initial efficiency was very low due to the limited harvesting of sunlight to the UV absorption range of TiO_2, a narrow portion of the solar spectrum.[12] Assembling semiconductor oxides with smaller bandgaps to extend the absorption to the visible (Vis) region may partially solve this issue but goes in the opposite direction of having conduction (CB) and valence (VB) bands of the required energy to drive reduction to hydrogen and oxidation to oxygen (0.00 and 1.23 V vs NHE at pH = 0, respectively). Scaife in 1980 pointed out the limits in finding this compromise due to the deeply positive level of the valence band constituted by the O-2p orbitals.[13] Since then, tremendous efforts have been dedicated to improve Vis light harvesting by doping TiO_2 with non-metal, such as C, N, B, F,[14] and metal[14a] elements, or by the addition of plasmonic nanoparticles, Au in particular.[15] While this approach had partial success, since the presence of localized intra-bandgap states induced by many non-metal dopants actually enhances Vis light with positive effects on the photodegradation activity of the materials, it has little or no effect on hydrogen production as the modification does not alter CB edge position.[14b] Although black reduced TiO_2 showed very promising photocatalytic activity,[16] stability issues are still under investigations. Furthermore, TiO_2 engineering has been deeply investigated by preparing monodispersed nanocrystals[17] to understand the role of nanostructures in hydrogen production. In addition, nanocomposites and hybrid systems, with particular attention to combination of TiO_2 with carbon nanostructures, such as carbon nanotubes,[18] carbon nanocones,[19] or graphene[20] is well documented to have very positive effects in hydrogen photoassisted production thanks to the beneficial effect of enhancement of surface area with increased light absorption and increase of photogenerated charge carrier lifetime.[21]

An alternative approach to extend the portion of the harvested solar irradiation by the photoactive system is the use of colored dyes capable to absorb in the Vis wavelength range. In contrast to directly manipulating the optical properties of semiconductor, the dye acts exclusively as a photosensitizer, or antenna, with the main duty of efficiently absorbing the Vis light and then triggering the remaining steps of the water splitting process. In this way the light harvesting, charge transport, and photocatalytic reaction steps are separated and performed by different components, which can be optimized in their specific role. This option recently attracted the interest of many research groups since it is the common strategy adopted by other more mature solar technologies, such as dye-sensitized solar cells (DSSC).[22] The judicious exploitation of the multiyear investigation of sensitizers for DSSC and the extension of that knowledge to the target of hydrogen dye-sensitized solar production is therefore an attractive field of research.

Artificial photosynthesis and water splitting represent a very large field of investigation, spanning from inorganic and organic chemistry to biological and bio-inspired systems. In a photocatalytic device light is absorbed (directly or through a photosensitizer) and the electrons and holes reduce water to hydrogen and oxidize water to oxygen, respectively. One critical drawback is that hydrogen and oxygen are produced in the same environment and easily recombine before they can be separated. Furthermore, when testing new materials, it is advantageous to focus investigation to only one semi-reaction, either reduction or oxidation. Therefore, one common approach is to limit the process to either reduction to hydrogen or oxidation to oxygen in the presence of a sacrificial electron donor (SED) or acceptor (SEA), respectively. In fact, SED and SEA play the role of hole and electron scavengers, respectively, in place of water in the water splitting half-reaction which is omitted (Figure 2).[9]

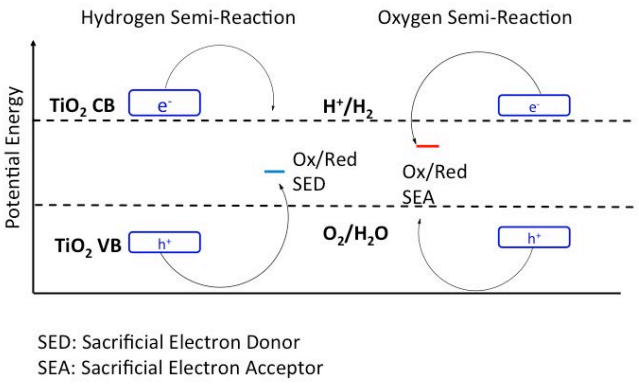

Figure 2: Hydrogen or oxygen production in the presence of sacrificial agents.

Since this paper focuses interest on the use of organic sensitizers, we decided to limit this review to photocatalytic systems where the semi-reaction of the reduction to hydrogen is investigated, that is the water splitting sector where organic dyes have been mostly used. In this half-reaction, the working mechanism reminds the DSSC process. Following light harvesting, dye excitation, and injection of the photoelectrons in the CB of the semiconductor oxide, electrons are transferred to the electrode and to the external circuit to produce electricity in DSSC, whereas electrons in the TiO_2 CB reach the active reaction center (reduction catalyst) to generate H_2 (chemical

energy instead of electrical energy) in the photocatalytic system. Figure 3 illustrates the two working mechanisms, with the shared features highlighted in violet.

Bianca Cecconi was born in Florence, Italy. She received her Master Degree in organic chemistry (2012) from the University of Florence under the guidance of Dr. Alessandro Mordini, working on heteroaromatic metal-free sensitizers for dye-sensitized solar cells. In 2013 she joined the PhD program in materials science at the University of Milano-Bicocca under the guidance of Prof. Abbotto, working on photocatalytic hydrogen production.

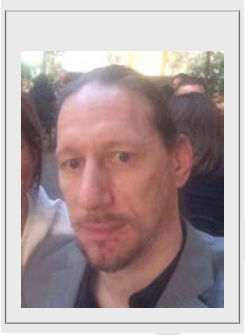

Norberto Manfredi. was born in Milan, Italy. He received his Masters degree in Materials Science from the University of Milano-Bicocca, Italy, in 2005 with Prof. G. A. Pagani studying heteroaromatic materials for non-linear optics and electrocromics. In 2008 he joined the group of Prof. Abbotto working on the synthesis and development of organic photovoltaic devices and photocatalysis. He is currently involved in the Milano-Bicocca Solar Energy Research Center (MIB-SOLAR).

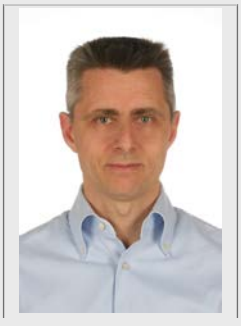

Paolo Fornasiero is associate-professor in Inorganic Chemistry at the University of Trieste. He received the 2005 Nasini Medal and the 2013 Chiusoli Medal from the Italian Chemical Society and the 2016 Heinz Heinemann Award from the International Association of Catalysis Societies for his contribution to inorganic chemistry and catalysis. His main research interests are in materials for energy and environmental related applications.

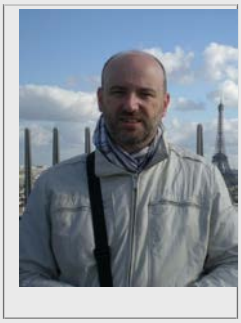

Tiziano Montini is assistant professor in Inorganic Chemistry at the University of Trieste. In 2012, he received the “Alfredo di Braccio” prize from Accademia Nazionale dei Lincei and the 4th Jonior ERES Award by the European Rare-Earth Society. His main research interests are in the design of heterogeneous catalysts for renewable valorization.

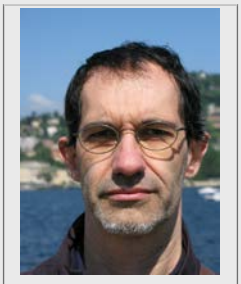

Alessandro Abbotto is full-professor of Organic Chemistry and Organic Materials and director of the Solar Energy Research Center MIB-SOLAR at the University of Milano-Bicocca. He is member of International Advisory Board of EurJOC. He coordinates the interdivisional group of Chemistry of Renewable Energies (EnerCHEM) of the Italian Chemical Society. His main research interests are in materials and devices for solar energy.

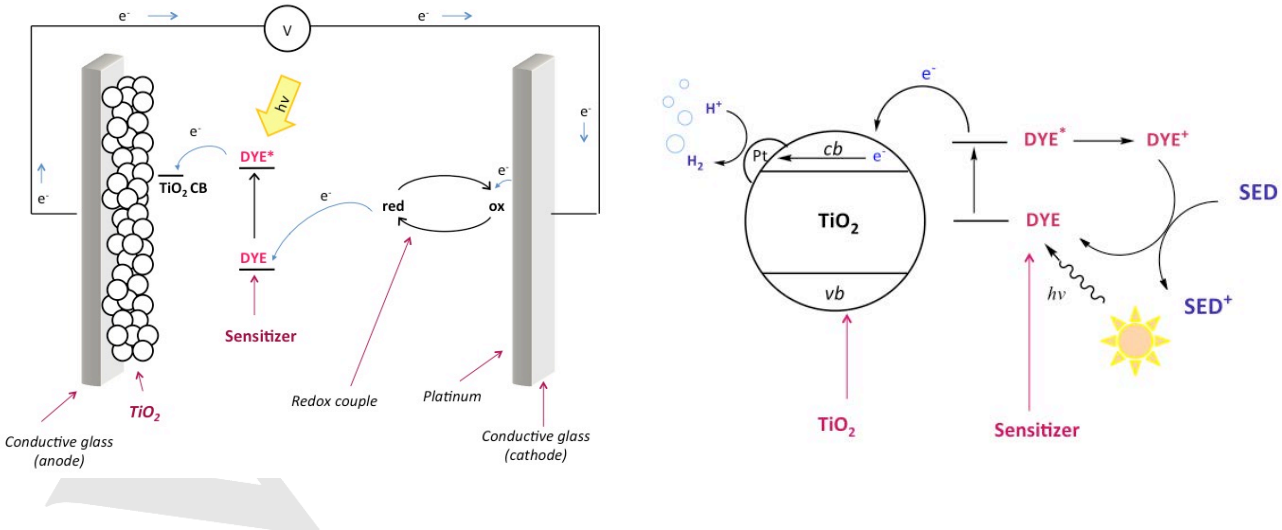

Figure 3: Comparison between the working mechanisms for electric (left) and chemical (right) energy production.

In a typical photocatalytic system for the dye-sensitized reduction of water to hydrogen using Pt/TiO_2 as a catalyst, the involved steps are as follow:

$$Pt/TiO_2/Dye \xrightarrow{h\nu} Pt/TiO_2/Dye^* \quad (1)$$

$$Pt/TiO_2/Dye^* \longrightarrow Pt/TiO_2(e^-)/Dye^{+\cdot} \quad (2)$$

$$Pt/TiO_2(e^-)/Dye^{+\cdot} + SED \longrightarrow Pt/TiO_2(e^-)/Dye + SED^+ \quad (3)$$

$$Pt/TiO_2(e^-)/Dye + H^+ \longrightarrow Pt/TiO_2(e^-)/Dye + \tfrac{1}{2} H_2 \quad (4)$$

$$Pt/TiO_2/Dye^* \longrightarrow Pt/TiO_2/Dye^* + h\nu \quad (5)$$

$$Pt/TiO_2(e^-)/Dye^{+\cdot} \longrightarrow Pt/TiO_2/Dye \quad (6)$$

Dye is responsible for light harvesting and goes to an excited state upon the absorption of a photon (1) followed by electron injection into the CB of TiO_2, resulting in charge separation (2). To have an efficient process and high durability of the dye, fast regeneration from the SED agent must take place (3) recovering the dye starting redox state. Electrons are trapped on Pt(0) particles adsorbed on the TiO_2 surface and reduce water (H^+) to molecular hydrogen (4). A few detrimental paths can be present in the process, with two main steps responsible for loss in activity: relaxation of the dye to its ground state before electron injection to the CB of the semiconductor (5) and hole-electron recombination between TiO_2 and dye stimulated by slow H_2 generation and/or dye regeneration (6).

Though investigation of DSSC sensitizers has been largely covered in the last two decades,[23] following the first work by Grätzel and coworkers in 1991,[24] the interest in dye-sensitized hydrogen production is still restricted to much fewer reports. As for DSSC dyes, sensitizers for hydrogen photocatalytic production can be classified in three main categories: organometallic complexes, natural or bio-inspired dyes, and metal-free organic dyes. In this paper we have reviewed the investigation of organic dyes in photocatalytic systems for hydrogen production from water and sunlight, focusing attention on selected synthetic approaches of the most important families and structure/function relationships. One first main difference from DSSC dyes is the operational condition environment. In fact, whereas DSSC dyes should work in a typical organic medium, such as acetonitrile or other organic solvents, sensitizers for hydrogen production are designed to efficiently work in water or aqueous-based media.

After a description of the main parameters to evaluate the efficiency of a photocatalytic systems, the article first briefly summarizes the most important organometallic and nature-inspired dyes, and then describes in more details organic dyes, pointing out targets and properties of the molecular systems. In particular, we stressed the relationships between structural design, hydrogen production efficiency, and stability, with the aim to provide the reader with the appropriate tools for future design. Synthetic approaches have been included only for the most representative families of donor-acceptor organic dyes.

2. Operation Principles and Main Parameters for Performance Assessment

In order to properly describe the different classes of sensitizers and comparatively describe efficiency and main properties of the sensitizers in the production of hydrogen, we first introduce the most used and important parameters for performance evaluation. Most photocatalytic studies are performed in a suspension of dye-sensitized TiO_2 nanoparticles covered by Pt(0), typically deposited via impregnation[25] or photodeposition[26] from H_2PtCl_6 under UV irradiation. Dye staining is performed in a similar manner as in the fabrication of DSSC photoanode by typically suspending less than 1 g of Pt/TiO_2 nanopowders in a few mL of dye solution (e.g. mM solution in alcohol or other solvents) for a few hours in the dark, to prevent dye photodegradation. Nanopowders are then separated through centrifugation, washed with the used bath solvent, and dried. In order to estimate the amount of adsorbed dye, the concentration of the dyes in the residual staining solution can be ascertained by UV-Vis spectroscopy, to confirm the complete loading of dyes on the Pt/TiO_2 material or, alternatively, to determine the non-adsorbed quantity.

Once the dye/Pt/TiO_2 catalytic materials have been prepared, the nanopowders are suspended in an aqueous media containing the SED agent. Typical SEDs are triethylamine (TEA), triethanolamine (TEOA), and ethylenediaminetetraacetic acid (EDTA) though other inorganic (e.g., S_2^-, SO_3^{2-}, Fe^{2+}, Ce^{3+}, I^-, Br^-, and CN^-) and organic (alcohols, aldehydes, organic acids, amines) SEDs have been also investigated.[27] The pH of the reaction mixture is typically adjusted to neutral. The photoreactor is then evacuated from oxygen and irradiated with a Xenon lamp or a solar simulator provided with a UV filter at ~ 400 – 410 nm in order to cut off the UV portion of the irradiation and avoid direct TiO_2 excitation of electrons to the CB of the semiconductor. The produced hydrogen gas is finally quantitatively determined by using a gas chromatograph equipped with a thermal conductivity detector (TCD).

The amount of hydrogen evolved is recorded vs time and elaborated to give comparable entities (Figure 4a). The amount should typically increase with irradiation time unless dye deactivation takes place. Typical amounts are of the order of μmol, more rarely mmol. In order to check dye stability in terms of ability to withstand the production of H_2, gas evolution rates, reported as μmol h^{-1}, are also important (Figure 4b). In some cases, particularly for practical purposes, it is convenient to normalize the amount of evolved gas or the evolution rate to the weight of the catalytic powder (e.g. μmol h^{-1} g^{-1}). In this case comparison is meaningful only when catalysts with similar loadings of dye (that is, active sites) are considered.

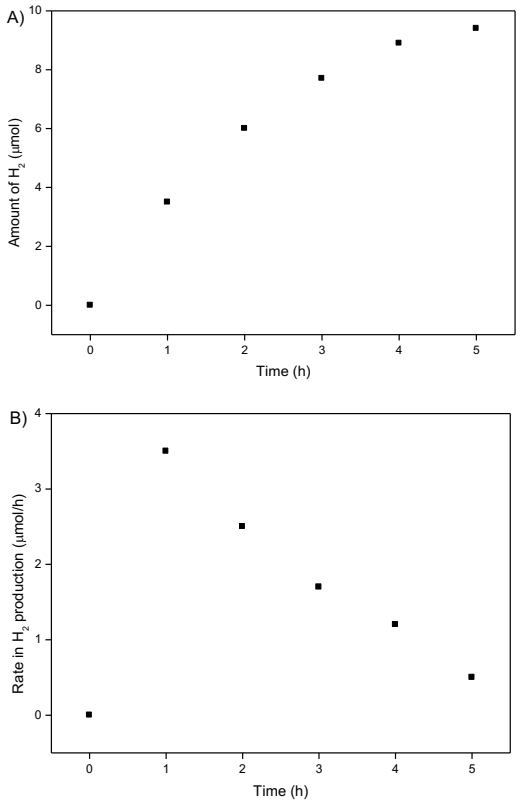

Figure 4: Elaboration of experimental data of a) amount of produced hydrogen vs irradiation time, and a) rate of hydrogen production vs irradiation time.

The first parameter to evaluate the ability of a photocatalytic system, in general, and in particular of a photocatalytic system to efficiently produce hydrogen is the Turnover Number (TON). In the reduction reaction from water to hydrogen, TON is the number of reacted electrons to hydrogen (which corresponds to the complete catalytic cycle), per active catalyst site, before the catalyst becomes inactive. Accordingly, the ideal catalyst would have an infinite TON. Indeed, in a catalytic process the equivalent molar amount of evolved hydrogen should always exceed that of the active photocatalyst. TON is described by Equation 2.

$$TON = \frac{number\ of\ reacted\ electrons}{number\ of\ active\ sites} \quad (2)$$

where the reacted electrons are those actually involved in the reduction from H_2O or H^+ to H_2. Since the number of active sites is difficult to directly determine, the alternative Equation 3 may be used.

$$TON = \frac{number\ of\ reacted\ electrons}{number\ of\ atoms\ in\ the\ catalyst} \quad (3)$$

In the specific case of dye-sensitized photocatalytic evolution of hydrogen, the catalytic active sites may be taken equal to the number of molecules of sensitizer and, considering that the number of reacted electrons is equal to (2 x molecules of produced H_2), the simplified expression Equation 4, where molecules have been replaced by moles, is used in practical experiments.

$$\mathrm{TON} = \frac{2 \times moles\ of\ produced\ hydrogen}{moles\ of\ dye\ on\ the\ nanoparticles} \quad (4)$$

Since the moles of evolved hydrogen are clearly dependent on how long the reaction is followed over time, TON is dependent on the irradiation period. Therefore each TON value should be always referred to the time scale (e.g. TON(5 h)). For this reason, the Turnover Frequency (TOF), that is rate per active site, can be also used. TON and TOF are also dependent on all the specific conditions of the catalytic reaction, in particular temperature, intensity of the light irradiation and presence of wavelength filters. Therefore, the quantum yield (QY) becomes the actual parameter to be used when comparing different catalytic systems. In this case, the number of catalytic sites is replaced by the number of photons. The external QY is given by Equation 5 or, in terms of evolved gas, by Equation 6, which is commonly used in photocatalytic experiments. This is an apparent quantum yield (AQY) since not all the incident photons are effectively absorbed and reach the reaction center. The external or apparent QY can be seen as the equivalent of the external quantum efficiency in photovoltaics (also known as IPCE in the DSSC literature).

$$AQY = \frac{number\ of\ reacted\ electrons}{number\ of\ incident\ photons} \quad (5)$$

$$AQY = \frac{2 \times number\ of\ hydrogen\ molecules}{number\ of\ incident\ photons} \quad (6)$$

To determine AQY, the number of incident photons must be measured, for instance by using a silicon photodiode placed in the photoreactor. Since this number can be relatively easy to determine for a single wavelength, AQY is typically reported as a function of the wavelength using a monochromatic light source (or through band-pass filters). In comparative studies, AQY is usually reported at the same wavelength though a more reliable value should be the AQY referred to the maximum of the Vis absorption of the dye-sensitized photocatalyst, which obviously varies with the specific dye sensitizer.

The intrinsic or internal quantum yield IQY, where the absorbed photons actually reaching the active site are considered, is given by Equation 7. IQY is the corresponding parameter to the internal quantum efficiency, also known as APCE in the DSSC field, for PV systems. The real number of absorbed photons, that is the real number of photons involved in the catalytic cycle, is not easy to determine in an heterogeneous mixture constituted by the dye/Pt/TiO_2 suspension in water, because of light scattering. This parameter is therefore rarely used.

$$IQY = \frac{number\ of\ reacted\ electrons}{number\ of\ absorbed\ photons} \quad (7)$$

It is evident that the measured AQY is, by definition, less, or at most equal to the real IQY, being the number of incident photons equal or larger than that of absorbed photons.

The most important efficiency parameter in PV is the power conversion efficiency PCE, or solar-to-electricity conversion efficiency (that is, produced electricity power over incident solar power). The corresponding parameter in dye-sensitized photocatalytic production of hydrogen is the Solar-to-Hydrogen energy conversion efficiency (STH), that is the efficiency of the system in terms of amount of the incoming solar energy converted to chemical energy in the hydrogen product (Equation 8), where F_{H2} is the flow of H_2 produced (expressed in mol s^{-1}), ΔG^0_{H2} is the enthalpy associated with H_2 combustion (237 x 10^3 J mol^{-1}), S is the total incident light irradiance (expressed in W cm^{-2}), and A_{irr} is the irradiated area (expressed in cm^2):

$$STH = \frac{F_{H_2} \times \Delta G^{\circ}{}_{H_2}}{S \times A_{irr}} \quad (8)$$

An alternative way to describe the conversion efficiency is the Light-to-Fuel Efficiency (LFE), as defined in Equation 9, where ΔH^0_{H2} is the enthalpy associated with H_2 combustion (285.8 x 10^3 J mol^{-1}):

$$LFE = \frac{F_{H_2} \times \Delta H^{\circ}{}_{H_2}}{S \times A_{irr}} \quad (9)$$

Both STH and LFE give an indication of the efficiency in conversion of solar energy into chemical energy stored in the form of H_2 and derive from photoelectrochemical studies, being calculated through the voltage, current, and the faradaic efficiency for hydrogen evolution.[28] However, STH and LFE values are still not commonly used in the research community and rarely reported in dye-sensitized hydrogen studies. It must be underlined that STH and LFE are dependent on the experimental conditions and the irradiation time. Therefore, comparison of STH and LFE between different studies must carefully check the adopted experimental conditions. Typical reported values of STH and LFE are below (in most cases much below) 1%, comparable to the low efficiency of the natural photosynthesis in biomass conversion (0.1-1%).[29]

Many studies have analyzed the effect of varying the reaction pH, the dye concentration on the TiO_2 surface, and the concentration of the suspension (amount of nanoparticles per volume of water) on the hydrogen production efficiency.[30] The pH of the medium affects the stability of the catalytic system and the availability of protons to reduction. The best pH trade-off for Pt/TiO_2 in presence of amines as SEDs is neutral. Dye concentration on the nanoparticles surface needs to be optimized as well. Light harvesting, and corresponding device efficiency, increase with dye loading until a maximum value is reached after that the efficiency starts to decrease. This effect is either due to the competition between light absorption and energy transfer and to detrimental intermolecular self-quenching phenomena. Depending on the dye structure and size, different optimal dye concentrations have been found. The optimal suspension concentration is a trade-off between higher efficiency light collection and lower decrease in the sunlight penetration depth typical of highly concentrated systems.

3. Organometallic Complexes

Ruthenium complexes play a prominent role in this class.[31] The vast literature on Ru(II) bis-2,2'-pyridine (bpy) complexes,[32] as well as their large use in DSSC[33] (where benchmark Ru(II) bpy derivatives N3-N719 had detained the record PCE for almost two decades[34] and several Ru(II) dyes have been designed and investigated)[35] has prompted many researchers to test them for hydrogen solar production. However, in spite of the high performances in DSSC, ruthenium complexes showed limited activity. When investigated in comparison with organic sensitizers, the latter often present better activities, in contrast with what commonly found in DSSC,[36] where only very recently record efficiencies have been communicated for DSSC sensitized by organic dyes.[37] As a representative example we cite the overall water splitting reaction in a PEC device investigated by Mallouk et al., who designed a ruthenium sensitizer with anchoring phosphonic groups to the TiO_2 surface and malonic endings to bind an oxidation catalyst oxide (IrO_2).[38] Porphyrins and phtalocyanines have been also investigated. Phtalocyanines are characterized by two main absorption bands, the Soret band in the UV/blue range and the Q-band in the red/near-IR (NIR) region, where ruthenium complexes and organic dyes rarely present strong absorptivities. Zang et al.[39] have investigated a class of zinc phtalocyanines aimed at improving the activity in the NIR region, achieving good results both in terms of gas evolution and dye stability. Here the authors designed asymmetric phtalocyanines such as **Zn-*tri*-PcNc** (Figure 5), characterized by a donor-acceptor structure in order to more efficiently generate the charge separation. In fact, the corresponding symmetric complex **Zn-*tetra*-Nc** is less active. Terminal *t*-butyl groups have been inserted to act as de-aggregating units.

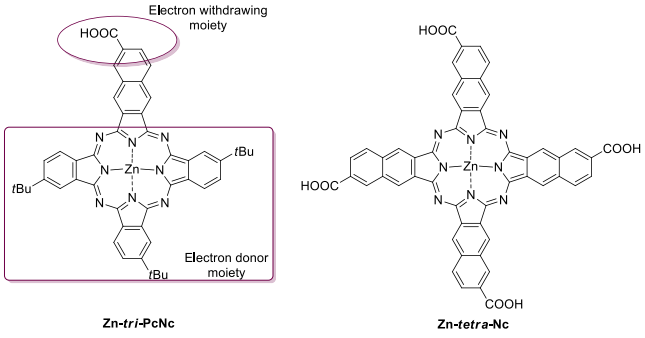

Figure 5: Structure of phtalocyanine dye Zn-tri-PcNc compared to the symmetric tested one Zn-tetra-Nc, push-pull structure is outlined in violet.

4. Organic Dyes: Emissive Molecules

A first class of organic dyes that has been largely investigated is that of emissive dyes, with particular interest on the fluorescent dye Eosin Y. In general, reports do not compare the photocatalytic activity of emissive vs non-emissive dyes. For this class of sensitizers, it appears more significant the effect of the excitation mechanism on the hydrogen generation and stability properties.

Two excitation mechanisms have been proposed (Figure 6): a) reductive quenching, in which the dye in its excited state accepts the electron from the SED after photon absorption, followed by electron injection to the CB of the semiconductor; b) oxidative quenching, in which the electron injection to the CB of TiO_2 precedes the regeneration from the sacrificial agent. In the first case, electron transfer to the semiconductor leaves the dye in its neutral state (dye) whereas in the latter the electron injection affords the dye oxidized form ($dye^{+\cdot}$). Examples of the dyes belonging to the two categories are shown in Figure 7.[40] Spectral characteristics of some of those dyes anchored on TiO_2 surface are listed in Table 1. In particular, we note that the emission peak is not affected by grafting onto TiO_2. For instance, the emission peaks of 622 and 540 nm of the TiO_2-anchored Thionine and Eosin Y, respectively, compare with the value of 622 and 546 nm for the same dyes in water.

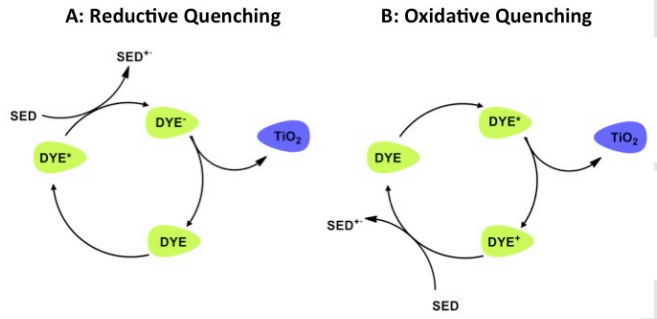

Figure 6: Schematic illustration of reductive and oxidative quenching.

Sensitizers belonging to the second class are more active in the photoinduced production of hydrogen as can be seen from Figure 8 and from the data listed in Table 2. One of their limitations is the low stability due to degradation pathways during the photocatalytic experiments. For instance, xanthene rings are easily hydrogenated in the H_2-Pt/TiO_2 environment, leading to inactive non-conjugated molecules. *Ortho*-dihydroxyl-anthraquinones such as Alizarin and Alizarin Red showed higher stability[41] compared to the more common dyes Eosin Y[42] and Coumarin 343 in the strongly reducing environment present during irradiation. For these scaffolds the undesired hydrogenation of the conjugated core leads to the formation of hydrogenated anthraquinones, which are no longer active in an anaerobic environment. However, they are able to recover the original active form by contact with oxygen. Thus, in these cases a temporary deactivation is observed in place of the permanent degradation typical of Eosin Y and Coumarin 343.

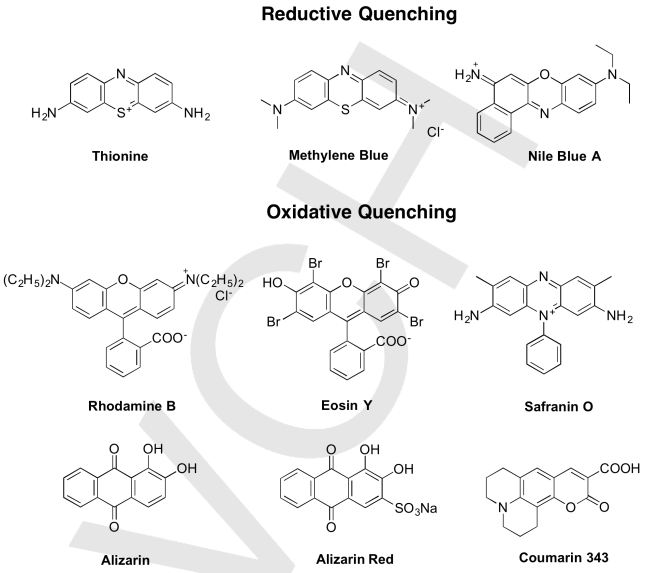

Figure 7: Selected emissive dyes.

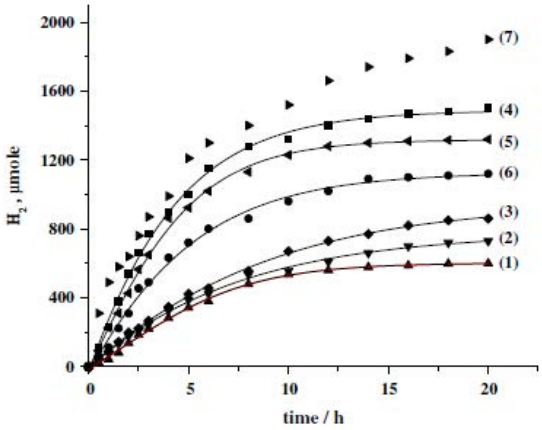

Figure 8: Photoproduction of H_2 vs time for various dye modified unplatinized TiO_2 photocatalysts; 1) thionine, 2) methylene blue, 3) nile blue A, 4) eosin Y, 5) rhodamine B, 6) safranine O, and 7) eosin Y over TiO_2/Pt photocatalyst. Reprinted from ref., [40] copyright 2010, with permission from Elsevier.

Table 1: Characteristic spectral data (absorption and emission maxima) of some emissive dyes anchored on TiO_2.

Emissive Dye	λ_{max} (nm) Abs	λ_{max} (nm) Em
Thionine	602	622
Methylene Blue	663	679
Nile Blue A	643	675
Eosin Y	517	548
Rhodamine B	557	571
Safranin O	520	592

5. Organic Dyes: Donor-Acceptor Architectures. Main Design and Synthetic approaches.

Compared to emissive dyes, the donor-acceptor molecular architecture represents a more general approach for the design of organic sensitizers. Donor-acceptor structures are characterized by the presence of three sub-molecular units: an electron-donor (D), a π-spacer (π), and an electron-acceptor (A) group. The D-π-A framework has been often used in material science since it is associated to efficient charge separation. Indeed, this geometry has been extensively exploited for the design of DSSC sensitizers.[36a, 43] Donor-acceptor dyes follow an oxidative quenching mechanism (Figure 6). After electron donation from the excited state, the residual hole of the oxidized dye (dye^+) resides in the HOMO, localized in the D moiety. Therefore, the D group should lie as far as possible from the TiO_2 surface in order to prevent electron back-donation (charge recombination), and as close as possible to the SED in order to favor dye regeneration. π-Spacers are generally polarizable conjugated aromatic and heteroaromatic groups that are able to efficiently transfer charge and extend the π-conjugated framework for improved optical properties and light harvesting. The careful selection of the spacer unit is also associated to the stability of the dye under irradiation. Lastly, the A group is constituted by a strong electron-withdrawing functionality, able to efficiently withdraw electrons from the donor unit by resonance effect and promote charge separation upon photon absorption. The molecular LUMO, from where electron injection to TiO_2 takes place, is typically located in the terminal A component. The A group is often associated to an anchoring functionality to covalently graft the molecule to the catalytic center (e.g. Pt/TiO_2). Accurate energetic levels are required for the HOMO/LUMO of a sensitizer. In particular, the energy of the LUMO should be higher (that is, more negative vs NHE) than the CB of the semiconductor (-0.5 V vs NHE)[44] to allow electron donation. The level of HOMO should be lower (more positive vs NHE) than the redox potential of the SED to permit dye regeneration. Ab-initio computations, mostly using the DFT method, have been used to predict with good accuracy molecular orbital shapes and energies, thus allowing efficient pre-screening of sensitizers before carrying out their synthesis. Experimental HOMO and LUMO energies can be determined electrochemically from the oxidation and reduction potentials, respectively, measured either by cyclic voltammetry (CV) or differential pulsed voltammetry (DPV).[45] The difference between the oxidation and reduction potential defines the electrochemical energy gap. If the oxidation or reduction potential cannot be measured by CV or DPV, the optical band-gap, obtained by the absorption onset values using the Tauc plot [46] can be used. Electrochemical and optical bandgaps are used to evaluate the HOMO-LUMO gap of the dye. In the following sections the most important donor-acceptor sensitizers tested in dye-sensitized photocatalytic hydrogen production will be presented. The molecules are classified according to the chemical nature of the D core: a) triarylamines; b) phenothiazines; c) other D moieties. Molecular design and selected synthetic approaches will be presented for each class of sensitizers.

5.1. Triarylamine dyes

Dyes incorporating the common triarylamine (TAA) Ar_3N core have been by far the most studied systems.[47] Dyes are depicted in Figure 9. The design of TAA-based dyes has been focused on the following aspects: a) modification of surface wettability (hydrophilicity) without interfering on the conjugated skeleton of the molecule (dyes **1** – **7**); b) modification of the π-spacer with the introduction of groups of varying length of the π-system (dyes **8** – **12**); c) modification of the chemical nature of the π-spacer (dyes **13** – **14**); d) modification of the number of acceptor and anchoring units (dyes **15** – **17**).

Hydrophilic dyes have been introduced with the aim of increasing the wettability surface of TiO_2 nanoparticles in aqueous solutions. Indeed, whereas liquid DSSC are based on electrolytes in organic solvents (e.g. acetonitrile), the presence of an aqueous medium in the case of the photocatalytic hydrogen production requires modification of the solubility properties of the organic dyes, which are intrinsically hydrophobic due to the chemical nature of the constituting units. Poor affinity to water could negatively affect the behavior of the dyes at the interface with the medium and consequently disfavor charge transfer and chemical steps involved in the whole process. The introduction of glycolic chains with different length and their effect on hydrogen production efficiency have been investigated. The first kind of modification considered the length of a glycolic chain in the *p,p*' sites of the terminal phenyl rings of Ar_3N (dyes **1** – **5**).[30b] A second study compared the effects of introducing the hydrophilic chains in the donor vs the middle spacer unit (dyes **6** and **7**).[48] The distance of the hydrophilic groups from the TiO_2 surface could differently affect process mechanisms. For example, introduction of the substituents on the terminal D moiety mostly affects the interaction of the sensitizers with SED. The general synthetic route for the synthesis of hydrophilic dyes is illustrated in Scheme 1. Metal-catalyzed cross coupling reactions[49] are by far the most favorite reactions to link aromatic cores pre-substituted by the hydrophilic chains. The convenient use of synthetic precursors bearing glycolic chains is possible since the presence of these groups is compatible with the cross-coupling conditions.

A second design strategy is centered on the π-spacer, due to the important contribution of this group to light harvesting properties and additional features, such as photochemical stability. Dyes **8** – **10** showed the expected optical properties trend in correspondence with π-framework elongation (see Paragraph 6). A similar trend is observed for dyes **11** and **12** (synthetic pathways for dyes **11** and **12** are given in Scheme 2). Here the insertion of a polycyclic ring as a spacer (cyclopenta[2,1-*b*:3,4-*b*']dithiophene, CPDT) has been associated to an extended conjugated path in the donor core, where the Ar_3N core has been decorated with electron-rich aryl groups.[30e] In particular, the presence of the four terminal alkoxy substituents has the role of enhancing the donor character to promote charge separation, de-aggregating the conjugated molecules to prevent self-

quenching of the excited state, and protecting the TiO_2 surface from charge recombination to SED. This substitution pattern has been already introduced with success by Hagfeldt et al.[50] in the DSSC technology to retard recombination and boost the use of cobalt-based redox couples to afford record PV efficiencies of nearly 15%.[37b]

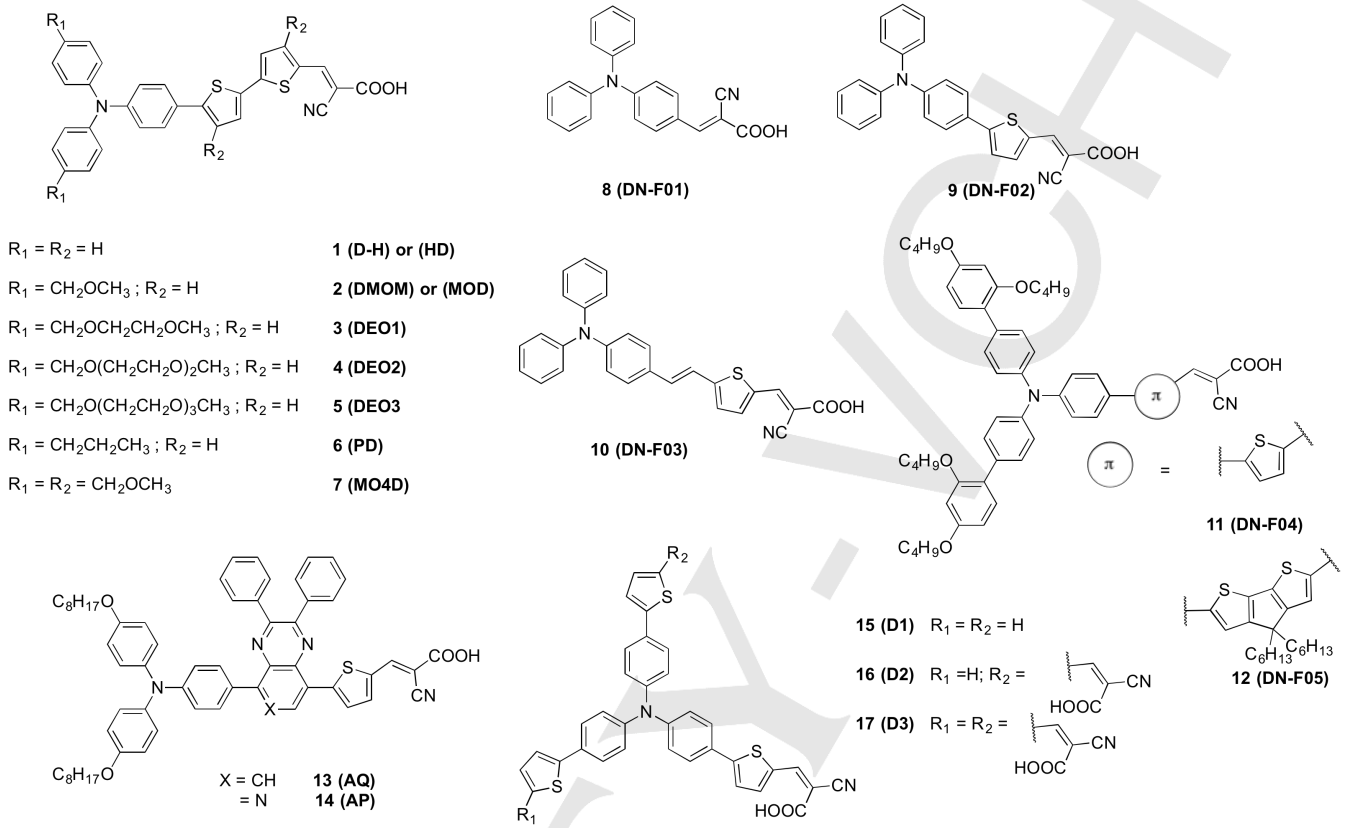

Figure 9: TAA-based sensitizers.

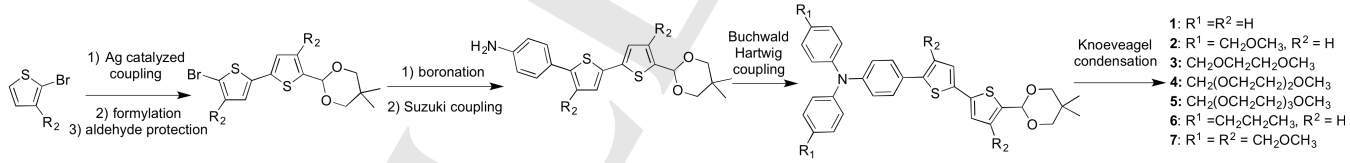

Scheme 1: Synthetic route to TAA-based hydrophilic dyes **1 – 7**.

An alternative approach has been proposed by Tian et al. with the introduction of an auxiliary acceptor A' in a D-A'-π-A skeleton, in order to enhance charge separation and electron injection.[51] The A' quinoxaline (in dye **13**) and pyrido[3,4-*b*]pyrazine (in dye **14**) groups have been investigated. As in the case of hydrophilic dyes, metal catalyzed cross-coupling reactions, in particular a sequence of Suzuki-Miyaura reactions,[52] have been selected to build dyes in a divergent fashion.[53] In all of the presented examples, a final Knoevenagel condensation in either basic or acidic conditions is used to convert the aldehyde precursor groups into cyanoacrylic acids, which have been preferred as acceptor/anchoring units.

Park et al. studied the effect of varying the number of grafting units in anchoring geometries to TiO_2, and their corresponding hydrogen production activities (dyes **15 – 17**).[54] These dyes differ for the number of anchoring cyanoacrylic moieties. Only one anchoring mode can be envisaged (upright Y mode, see Scheme 3) for the mono-branched system **15**, whereas two geometries are conceivable for the di-branched dye **16** (upright Y and inversed Y modes). Lastly, three alternative modes are active for the three-branched system **16** (tripod, upright Y, and inversed Y modes). Dyes were synthetically accessed via a Stille cross-coupling reaction followed by a Vilsmeier-Haack formylation using different equivalents of $POCl_3$, to afford the mono-, bis-, or tris-aldehyde derivative. Aldehydes are finally converted to the corresponding cyanoacrylic acids through acidic Knoevenagel condensation (Scheme 3)

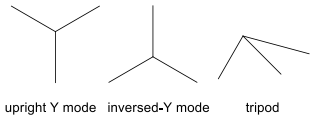

Figure 10: Anchoring modes to TiO_2 for dyes **15** – **17.**

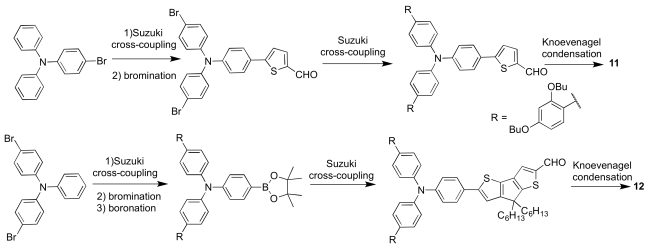

Scheme 2: Synthetic route to TAA-based dyes **11 – 12.**

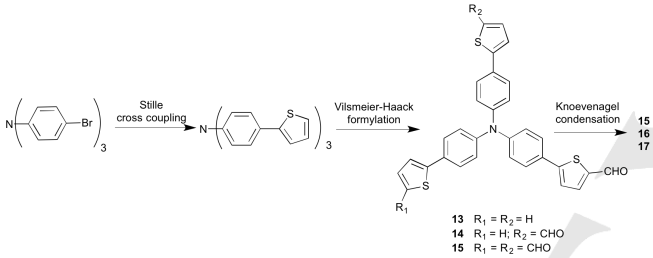

Scheme 3: Synthetic route to TAA-based hydrophilic dyes **15 – 17.**

Although not strictly belonging to the family of sensitizers presented in this section, we also introduce a family of donor-acceptor dyes where a *N,N*-dialkylanilino donor group has been fused with a coumarin acceptor moiety which is connected, though different vinylene and thiophene-based spacers, to the acceptor/anchoring cyanoacrylic end-group (Figure 11, dyes **18** – **22**). Using this interesting coumarin-based class of sensitizers, Abe et al. have investigated the overall water splitting photocatalytic process using for the first time a simple organic sensitizer on a $Pt/H_4Nb_6O_{17}$ semiconductor for H_2 evolution and a WO_3 photocatalyst for O_2 evolution.[55] The I^-/I_3^- redox shuttle was added to complete electrons circulation. In this work the authors screened different spacers with the aim of enhancing light harvesting as well as stability of the oxidized form of the dye. Such requisite is fundamental when the overall water splitting process is studied since, in absence of a SED, dye regeneration is slower and a poor stability of the dye radical cation could spoil the whole process.

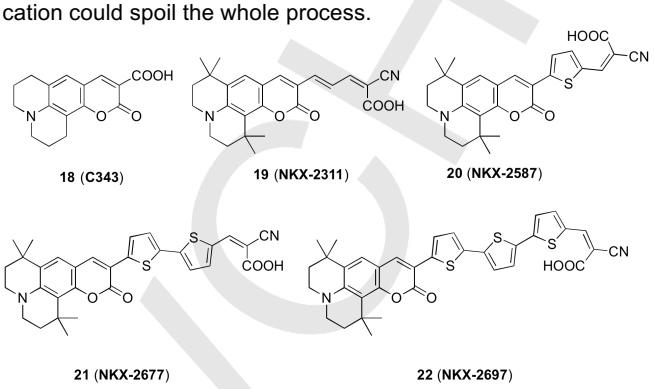

Figure 11: Coumarin sensitizers.

5.2. Phenothiazine dyes

An increasing number of studies have recently used the phenothiazine (PTZ) core in dye-sensitized solar energy applications. The examples here referred to the photocatalytic hydrogen production follow the numerous applications in the DSSC field.[56] Indeed, the PTZ core carries peculiar features associated to its non-planar butterfly conformation along the S-N axis. This arrangement helps to minimize the negative effects associated with self-quenching molecular aggregates on the TiO_2 surface. PTZ contains two symmetric benzene rings, which can be conveniently functionalized allowing the design of symmetric di-branched dyes, a class of photosensitizers possessing higher anchoring stability and electron injection efficiency, improved optical properties, and enhanced device stability, as introduced by some of us in the DSSC field[57] and later used by many research groups.[58] Furthermore, the nitrogen atom of the central heteroaromatic ring can be conveniently functionalized in order to tune additional properties, such as proper solubility in specific media (e.g., water) or affinity to bio-inspired molecules. Finally, compared to other donor groups, this ring is very stable in its radical cation form, thus facilitating the electron donation and the stability of the system up to the regeneration by SED.

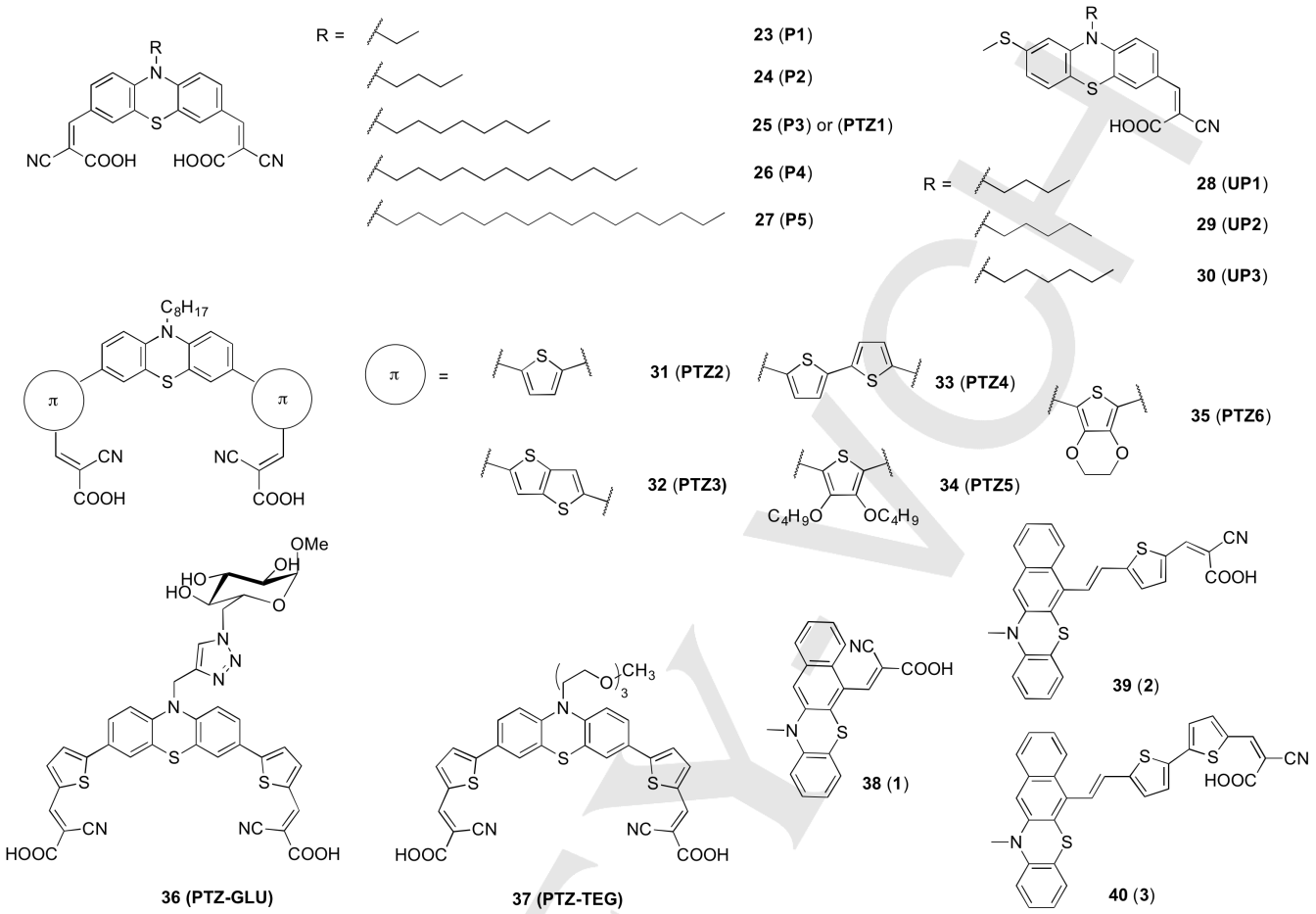

Figure 12: Phenothiazine-based sensitizers.

PTZ-based dyes used for the dye-sensitized evolution of hydrogen are summarized in Figure 12. The first two works presented here have investigated the effect of the varying length of the *N*-substituted alkyl chain on the hydrogen production efficiency. The early work by Son et al. varied the alkyl substituent in di-branched PTZ dyes from a 2- to a 16-carbon atom chain, with additional increments of an even number of methylene spacers (dyes **23** – **27**),[59] while a second article, where an alkylthio-substituted PTZ moiety has been used, has limited investigation to the smallest analogues (from butyl to hexyl chains in dyes **28** – **30**).[30d] The strategic role of introducing terminal alkyl chains to control dye aggregation and favor the right orientation on TiO_2 surface has been proposed.[30d] The synthetic access to dyes **23** – **30** implied alkylation of the PTZ nitrogen in basic conditions with the proper alkyl halide, followed by formylation under Vilsmeier-Haack conditions, and a final Knoevenagel condensation to introduce the A unit (Scheme 4, dyes **23** – **27**).

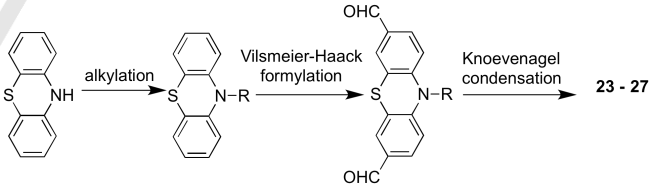

Scheme 4: Synthetic route to phenothiazine dyes **23** – **27.**

We have recently investigated the effect of the π-spacer on optical properties and, ultimately, hydrogen production performances.[60] Starting from dye **25** as a reference di-branched system, we have systematically varied the central unit using different mono-, poly-, and fused polycyclic thiophene-based groups (dyes **31** – **35**). These heteroaromatic rings have been selected amongst the most successful spacers exploited in organic and organometallic DSSC dyes[36a, 43] We have also screened the effect of using alkoxy-substituted electron-rich thiophene rings in dyes **34** and **35** to evaluate electronic and steric effects.

As for TAA derivatives, an important alternative to *N*-alkyl substituted PTZ-dyes is the design of hydrophilic dyes in order to improve water affinity and performance in aqueous media. As seen for TAA dyes, the most common strategy is the

introduction of a polyethylene glycol functionality, such as the widely used tris(ethylene glycol) monomethyl ether (TEG) group. In a recent work we have for the first time investigated the effect of introducing a peripheral glucose unit (**36**) to bust its affinity to water and enhance dye-sensitized photogeneration of hydrogen with respect to the glycolic derivative.[61] Indeed, compared to the corresponding alkyl derivative (**31**), as well as the triethylene glycol substitution (**37**), the sugar derivative showed a lower contact angle (Figure 13).

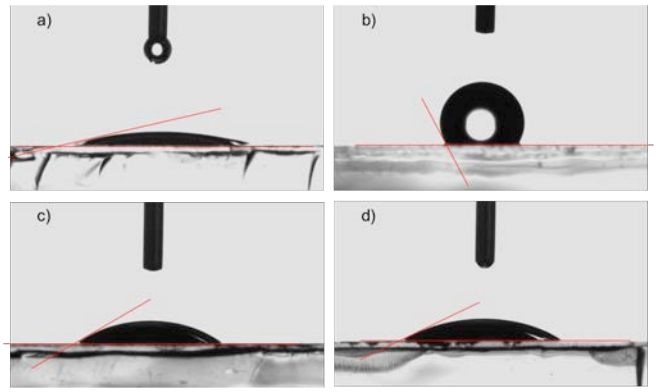

Figure 13: Cross-sections of a) a film of sintered TiO_2-NP; b) film of sintered TiO_2-NP sensitized with **31**; c) film of sintered TiO_2-NP sensitized with **37**; d) film of sintered TiO_2-NP sensitized with **38** and a drop of deionized water positioned on the top, which were used for the estimation of the contact angles (ϑc/°). Reproduced from ref., [61] with permission from The Royal Society of Chemistry.

The overall synthetic strategy to dyes **31** – **35** is depicted in Scheme 5. The Suzuki cross-coupling reaction has been selected to build the D-π fragment, introducing the boronic acid/ester either in the donor or in the spacer portion depending on the best synthetic availability. The synthetic strategy to dyes **36** is depicted in Scheme 6. The sugar functionality has been introduced by exploiting click chemistry and Cu-assisted azide-alkyne Huisgen cycloaddition. The D-π fragment has been built using a Suzuki cross coupling and the acceptor moiety has been introduced via Knoevenagel condensation.

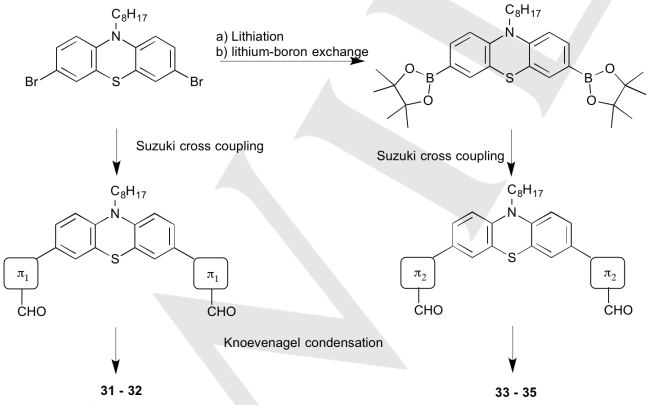

Scheme 5: Synthetic route to phenothiazine dyes **31** – **35.**

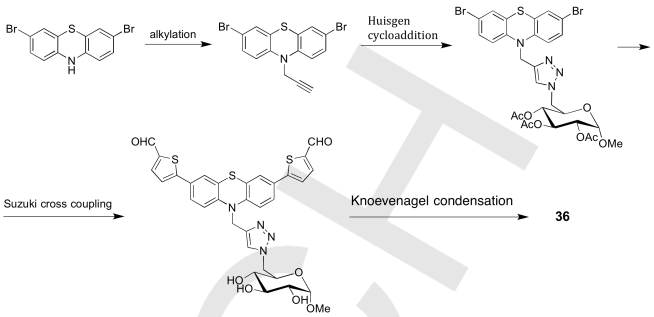

Scheme 6: Synthetic route to phenothiazine dye 36.

A series of mono-branched benzo[b]phenothiazine derivatives has been also investigated with the purpose of evaluating the effect of different thiophene-based spacers (**38** – **40)**.[62] The synthetic pathway to these dyes implied the use of a Wittig reaction between the phosphonium ylide of benzo[b]phenothiazine unit and the proper aldehydes (Scheme 7).

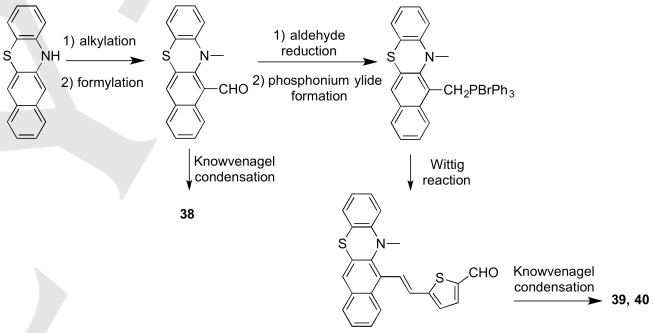

Scheme 7: Synthetic route to phenothiazine dyes **38** – **40.**

5.3. Sensitizers with other donor cores

A few other examples implying the use of donor cores other than TAA and PTZ have been reported. These examples are limited essentially to carbazole and dithiafulvalene D groups. The corresponding dyes are depicted in Figure 14. Despite the fact that the carbazole group has been extensively investigated in the DSSC literature,[63] only two dyes (**41** and **42**) have been tested for sun-driven hydrogen production.[30a] Whereas sensitizer **41** has a very simple structure, constituted by the direct connection of the carbazole group to the cyanoacrylic A unit, **42** contains a 2,2':5',2'':5'',2'''-quaterthiophene spacer, with each thiophene ring carrying an hexyl chain to improve solubility and prevent intermolecular aggregation. The carbazole dye **42**, also known as MK2, has been used with success as a DSSC sensitizer[64] and in particular in aqueous DSSC.[65]

The last reviewed examples contain a less common D core, rarely used even in DSSC studies. Dyes **43** and **44** are characterized by the presence a dithiafulvalene unit as a D moiety and a diketopyrrolopyrrole (DPP) based spacer. The two dyes differ by the presence of two alternative acceptor/anchoring groups (cyanoacrylic and malononitrile).[30c] Indeed, the

dithiafulvalene group is endowed with a high thermo- and photo-stability.[66] The thiophene-based spacer fragment contains a diketopyrrolopyrrole group, which has been widely used in pigments for paints and inks and investigated both in DSSC sensitizers[67] and donor polymers for organic PV.[68] The synthetic route, illustrated in Scheme 8, again exploits the Suzuki reaction to build the central thiophene-diketopyrrolopyrrole unit carrying two terminal formyl functionalities. A Horner-Wittig reaction followed by a Knoevenagel condensation binds the key bis-aldehyde intermediate to the D and A units, leading to the final molecule.

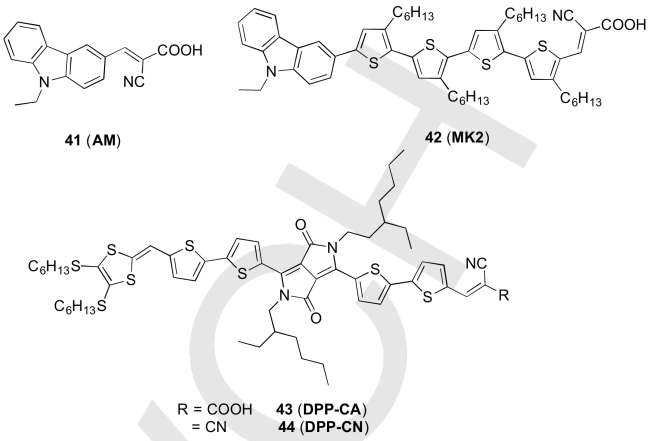

Figure 14: Carbazole and dithiafulvalene sensitizers.

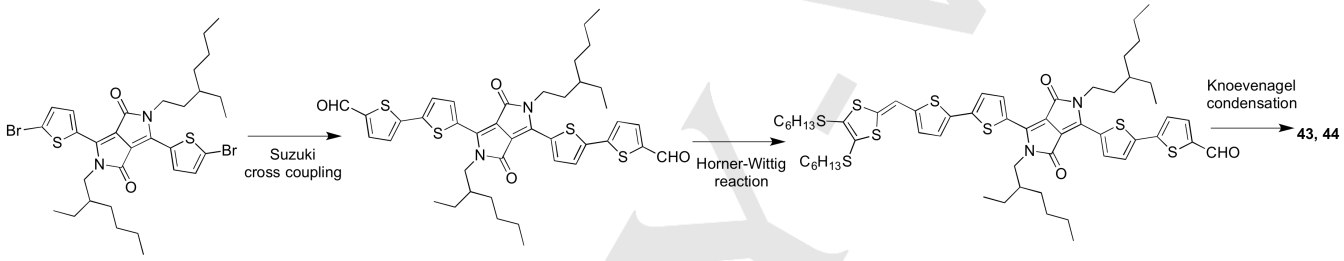

Scheme 8: Synthetic route to dithiafulvalene dyes **43** and **44.**

6. Donor-Acceptor Organic Sensitizers: Molecular Properties and Hydrogen Evolution Activity

Papers on dye-sensitized hydrogen production typically report a detailed optical and electrochemical study in order to validate molecular design and provide a rationale for measured efficiencies. The relevant data have been collected in Table 2. Optical properties mostly originate from the structure of the π-framework and are directly associated to the ability of the dye to harvest light. In general, donor-acceptor dyes show a classical pattern, with an intense absorption band in the Vis region attributed to the intramolecular donor to acceptor charge-transfer transition (ICT). When a side-substitution does not involve the π-conjugated backbone, optical properties are almost unvaried, as in the case of dyes **1** – **7**,[30b, 48] and **36** and **37**, where the introduction of hydrophilic groups on arylamines and phenothiazines, respectively, has been investigated, or of dyes **23** – **30**,[30d, 59] where the terminal alkyl chain has been varied.

When the comparative studies involve the design of the π-conjugated framework, molecular optical properties, and in turn light harvesting abilities, are significantly affected. The general behavior is the presence of bathochromic and/or hyperchromic effects upon inserting longer π-conjugated spacers. This important property is compatible with the use of thinner nanocrystalline films as those required by solid-state devices.[69] The qualitative and quantitative optical trend is clearly exemplified in the case of dyes **8** – **12**,[30e] where the introduction of thiophene-based spacers of increasing length is translated to a steady enhancement of light absorption both in terms of red-shifted maximum wavelength and molar absorptivities (Figure 15). In the case of dyes **15** – **17** the strong bathochromic effect on going from **16** to **17** is likely due to the symmetric arrangement of the acceptors in the latter dye. The increase of the conjugation path is responsible for the ε trend **15** < **16** < **17**.[54]

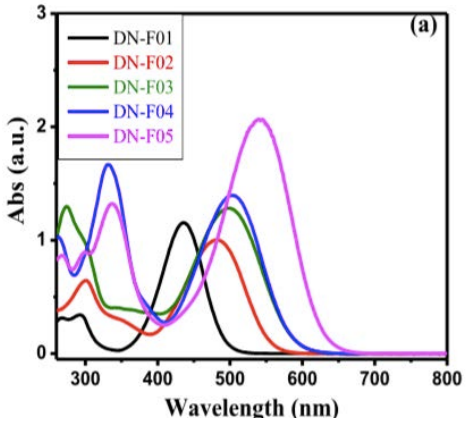

Figure 15: UV/Vis absorption spectra of dyes **8-12.** Reprinted from ref., [30e] copyright 2015, with permission from Elsevier.

A similar rationale, and design validation, is referred to the di-branched **31** – **35**,[60] recently reported by us, and mono-branched families **38** – **40**,[62] where again elongation of the π-spacer afforded enhanced optical properties. Figure 16 shows the absorption spectra of dyes **31** – **35** in THF solution. The spectra have been plotted against the molar extinction coefficient to better appreciate the strong hyperchomic effect upon elongation of the central thiophene unit. In our study we have shown that even the introduction of a single thiophene ring in compound **31** afforded a molar extinction coefficient twice larger than that in the reference system **25** (from 13 700 to 34 000 $M^{-1}cm^{-1}$) and a 11-nm red-shifting of the absorption peak. The use of spacers with longer conjugation paths confirmed this optical trend reaching molar absorptivities up to 60 000 $M^{-1}cm^{-1}$ as in **32** and **33**, that is more than four times larger than that **25**, and absorption peaks at significantly longer wavelengths.

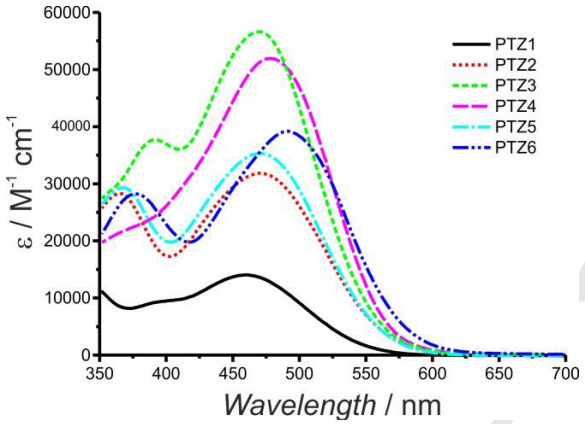

Figure 16: UV/Vis absorption spectra of dyes **31 – 35.** Reprinted from ref., [60] with permission. Copyright 2015 Wiley-VCH.

Apart spacers based on the efficient and thermally stable thiophene ring, other heteroaromatic rings have been explored in order to enhance the optical properties. For instance, in dyes **13** and **14** the introduction of the auxiliary acceptor quinoxaline or pyrido-[3,4-*b*]pyrazine afforded broad absorption bands in the Vis region both in solution and on 4-μm TiO_2 film.[51] The dyes exhibited two major bands, one in the 400 - 450 nm region due to the charge transfer from the TAA donor to the auxiliary acceptor A', and the other at 490 - 540 nm, attributed to the ICT band involving the cyanoacrylic acceptor. The ICT band appeared more red-shifted (533 nm) in the case of the pyrido-[3,4-*b*]pyrazine derivative.

The optical properties of the sophisticated dye **44** are impressive.[30c] Here the combined use of a DPP-based spacer and the malononitrile A moiety afforded an intense and broad ICT band over the whole Vis range (500 - 800 nm), with an absorption maximum at 674 nm in CH_2Cl_2 solution and a highly enhanced molar absorptivity, exceeding 1 x 10^5 M^{-1} cm^{-1} (Figure 17).

In particular, the presence of the bis-cyanovinyl acceptor in place of the conventional cyanoacrylic group caused a red-shift of 23 nm of the absorption peak and an almost twice larger ε. Thus the presence of the malonitrile acceptor is highly beneficial in terms of light harvesting abilities though this effect is counterbalanced by the weaker linkage with TiO_2, since the absence of the carboxylic group does not allow the formation of a stable ester bond with greater binding energies.

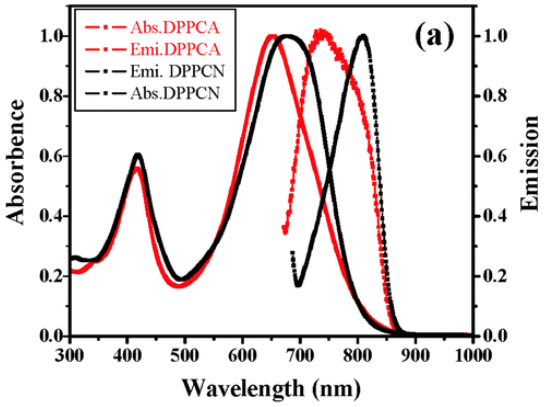

Figure 17: UV-vis absorption spectra of **43** and **44** in dichloromethane. Reproduced from ref., [30c] with permission from the PCCP Owner Societies.

As introduced in Section 5 HOMO and LUMO energy levels are important factors to efficiently generate hydrogen. Table 2 lists HOMO and LUMO energies (vs vacuum), when available from reports. Indeed, the energy of LUMO is always higher (more negative vs NHE) than the aforementioned level of the CB of the semiconductor. This property, in combination with a proper life time of the excited state, is a pre-requisite for efficient electron donation to TiO_2.[30b, 40, 51] Typically, a potential difference between the dye LUMO and the TiO_2 CB is required for efficient electron donation. This is the same requirement as for DSSC.[22b] It has been reported that values of LUMO around -3.0 — -3.6 eV are optimal for the thermodynamically feasible electron injection from the dye to TiO_2. In some cases, LUMO energies as low as -3.7 eV have been measured (see Table 2). Thus, it is apparent that a minimal offset of 0.3 eV between the LUMO of the dye and the CB of TiO_2 is the required minimum driving force for fast electron injection. Furthermore, LUMO of the dye should be localized as close as possible to the semiconductor surface, that is near the anchoring group (usually a carboxylic or phosphonic acid functionality). This has been often supported by computational studies at DFT level of theory.[51,59,62]

The HOMO level is also strategic for the whole mechanism since dye regeneration at acceptable rates is required in order to guarantee efficient activity and recurrence of the catalytic cycle. As described, the redox potential of SED must match the HOMO level of the dye and, in particular, the HOMO of the dye should lie below the energy level of SED. The redox potential of EDTA (-0.01 V vs NHE, -4.4 eV vs vacuum) is more negative than that of TEOA (+0.97 V vs NHE, -5.5 eV vs vacuum).[54] This means that dyes with a HOMO energy higher than -5.5 eV should require EDTA as a SED in order to provide efficient regeneration (see for instance dyes **1** – **5** in Table 2). In some cases collected in Table 2, the HOMO of the dye does not lie below the

redox level of TEOA as a SED, which could imply less efficient dye regeneration, though exact values might depend on the used solvent.

Choi at al. reported that the efficiency of photocatalytic activity using different SEDs, such as EDTA or TEOA, is not only related to the different redox potentials.[54] In fact, despite the different potentials exhibited by the two different SEDs, the photocatalytic activity is also affected by the electron transfer kinetics which are associated to the molecular interaction among dyes, TiO_2 surface, and electron donors.

The molecular design is finally transferred to the production of hydrogen, which should be as efficient as possible both in terms of amount of evolved gas and stability under solar irradiation. The efficiency of this process begins with the ability of harvest sunlight, as assessed by the optical properties. This is only the first stage of the complex multi-electrons process, which involves, as subsequent steps, charge separation (requiring proper HOMO/LUMO dye levels) and electron transport to the catalytic center, where the reduction of H^+ to hydrogen takes place. Therefore, it is not always straightforward to correlate molecular properties and hydrogen production photocatalytic efficiencies. For this reason, absolute efficiency values, for instance in terms of STH, are not so important when different sensitizers are tested. Accordingly, care is focused on the comparative studies, where different dyes with specific modified molecular design are compared under the same experimental conditions. Accordingly, a comparative evaluation between different studies, in particular when significantly different molecular design and different experimental conditions are involved, is awkward.

In general, a molecular design is considered to be successful when promising optical and energetic properties are transferred to relatively enhanced amounts of produced H_2 and stability over time. In the former case studies mostly report relative produced amounts of gas and TON values. In contrast, STH efficiencies are rarely presented. Conclusions on mid- and long-term stability under photocatalytic activity are seldom possible since, with few exceptions,[60] tests have been followed just over a few hours, rarely more than 10 h.

Table 2 summarizes the relevant activities in hydrogen production using the herein reviewed sensitizers. Since the reported parameters in the papers do not always allow a uniform comparison among the results, TON values have been also estimated by us from published data when possible.

The affinity of the sensitizer to the aqueous medium is a critical point. The introduction of oligoethylene glycolic hydrophilic chains of increasing length and polar character in **1** to **4** resulted beneficial for the production of hydrogen.[30b] The authors attributed this effect to the fact that a higher interface affinity between the dye and the medium makes the dye regeneration from SED easier, since the SED (in this case, EDTA) dissolved in the aqueous phase can approach and interact more efficiently with the dye radical cation center. However efficiency was lower for **5**, the dye with longest triglyme chain. It is possible that steric effects inhibit the approach of EDTA to the radical-cation core and/or cover the Pt sites. When the glycolic chains are introduced in the π-spacer, as in dye **7**, the effect is adverse, suggesting that the arrangement of the solvent molecules around the dye is fundamental in the regeneration step, as highlighted in charge recombination studies through transient absorption spectra on TiO_2 films.[48]

As described in the previous section we have recently investigated a sugar derivative **36** of a multibranched organic sensitizer to evaluate whether the higher affinity towards water with respect to the corresponding dye **37** carrying the more conventional oligoethylene glycolic hydrophilic, as assessed by the aforementioned contact angle measurements, might be transferred to improved performances.[61] Indeed, the glucose dye **36** performed twice more efficient than **37** in the photogeneration of hydrogen both in terms of evolved gas (Figure 18) and turnover number. In this work, by carefully evaluating contact angle measurements, photocatalytic data, and by considering the structural peculiar features of the side substituents, we have concluded that the distinct behaviour of the new hydrophilic sensitizer is associated to the unique rigid, bulky, hydrophilic geometry of the glucose ring, where lower degrees of freedom and extra-wettability, favoring the interaction with reactants in aqueous solution and suppressing intermolecular quenching, cooperate to afford the higher efficiency. The general and scalable synthetic approach and the large variety of available mono- oligo- and polysaccharides might allow the access to a library of photosensitizers with finely tuned properties and potential to improve the efficiency of the production of solar fuels in water.

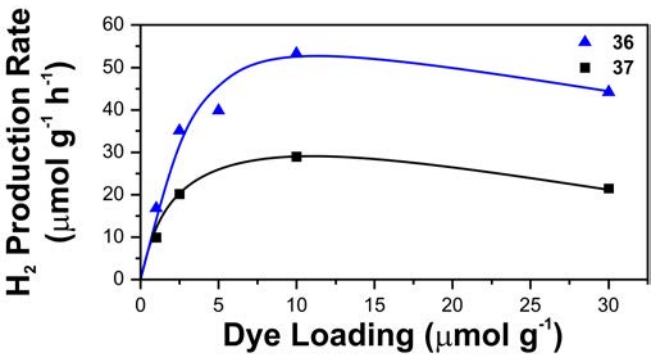

Figure 18: Production rates in H_2 evolution from TEOA 10% v/v solution at pH = 7.0 under irradiation with visible light (λ > 420 nm) using the Pt/TiO_2 materials sensitized with **36** and **37**.Adapted from ref., [61] with permission from The Royal Society of Chemistry.

The presence of hydrophobic alkyl chains similarly affected the photocatalytic activity. In the di-branched series **23** – **27**,[59] where different alkyl chains were introduced on the PTZ nitrogen atom, the photocatalytic activity improved as the length of the substituent increased (Figure 19). The dye **27** (**P5**) with an hexadecyl group showed, in presence of TEOA as a SED, the best activity after 5 h in terms of produced gas and TON (up to 1016). The beneficial effects of the longer alkyl chains have been justified with the effect of retarding the (self)quenching of the excited state and aiding the correct orientation of the molecules on the TiO_2 surface to favor electron injection.

Furthermore, the activity of the alkyl-substituted di-branched PTZ dye was higher than that of the reference emissive dye Eosin Y and of the Ru(II) complex N719 as well as of the corresponding mono-branched derivatives.

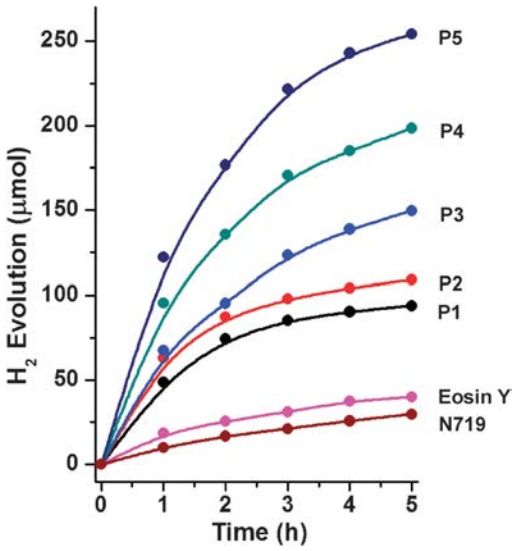

Figure 19: Hydrogen production profiles for dyes **23-27.** Reproduced from ref., [59] with permission from The Royal Society of Chemistry.

The modification of the π-conjugated spacer induced different effects on the photocatalytic efficiency. In some cases, the better optical properties yielded higher hydrogen production efficiencies, as in the case of the TAA dyes **8** – **12** (Figure 20).[30e] In the presence of TEOA, the photocatalyst sensitized by **12** (**DN-F05**), for which the best light harvesting properties were measured, exhibited the highest TON (1864) and an AQY of ~44%. The high TON supported the conclusion that the extension of the spacer length not only affected the amount of H_2 generation but also the stability of the dyes, as assessed by recyclability tests. The authors have hypothesized that the additional presence of the alkoxy and alkyl substituents in **11** and **12** provided an effective surface protection against electron recombination.

A valuable contribution has been given from the studies on D-A'-π-A dyes **13** and **14**,[51] containing the quinoxaline and pyrido[3,4-*b*]pyrazine auxiliary acceptors. The dye **14**, which showed the highest molar extinction coefficient, afforded a larger amount of hydrogen under Vis irradiation over 10 h using MeOH as a SED. The higher stability of the radical cation and the lower rates of recombination supported the higher activity. Interestingly, the photocatalytic activity was in agreement with the PCE in DSSC containing the same dyes. This work suggests that previous knowledge coming from DSSC studies, where a much larger literature exists, can be extended, with proper care, to the molecular design for hydrogen photogeneration.

When dyes **15** – **17** have been tested in the hydrogen production, the activity was found to be dependent on the selected SED. In the case of TEOA all the values were higher with a **17~16** > **15** trend.[54] The nature of the SED is supposed to affect the anchoring geometries of the di- and tri-branched dyes. The relative preference between the upright Y and inversed Y anchoring modes for **16** is apparently higher for the latter mode in the presence of TEOA. When EDTA is used as a SED, competitive grafting to the semiconductor takes place and the anchoring of the dye with only one cyanoacrylic moiety is preferred. Indeed efficiencies for **16** using EDTA are more similar to those associated to **15**, suggesting an upright Y anchoring mode. The most active dye is **17**, where the higher flexibility in the anchoring modes allowed the best performances of the series.

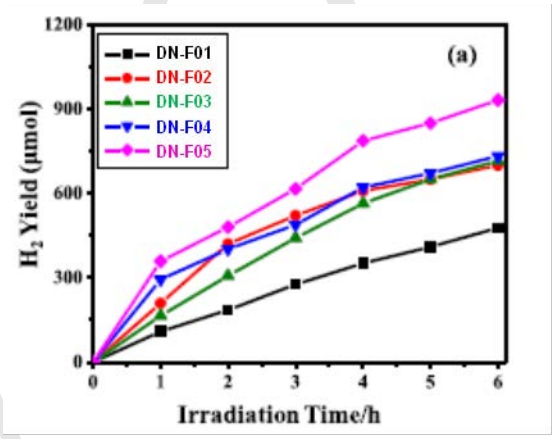

Figure 20: Hydrogen production profiles for dyes **8 – 12.** Adapted from ref.,[30e] copyright 2015, with permission from Elsevier.

We have recently systematically investigated the effect of inserting different thiophene-based spacers in the di-branched PTZ sensitizers **31** – **35** in the photocatalytic generation of H_2 (Figure 21).[60] In contrast with most studies, the activity has been followed for relatively long periods (20 – 90 h), in order to better evaluate long-term stabilities. The data from TEOA aqueous solution at pH = 7.0, under irradiation with Vis light (Figure 21a), were apparently in contrast with the results reported by the other groups. In fact, although the thiophene-substitution significantly improved the optical absorption properties, as discussed in the previous section, the amount of produced hydrogen per gram of catalyst was lower than that of the pristine dye **25** (Table 2). We attributed the lower performance to the strong and preferential interaction that sulfur atoms of the thiophene rings can establish with surface Pt atoms, inhibiting the catalytic activity by poisoning. However, when the rate of the hydrogen production has been considered (Figure 21b), the picture was significantly different. Firstly, the rate of production of the 3,4-dibutoxythienyl derivative **34** surpassed that of the reference dye **25** after 10 h. Note that this important outcome would could not be revealed if the study had lasted for a more commonly used shorter period. Secondly, while all of the thiophene-substituted sensitizers afforded rates progressively increasing with time, up to a constant value, the unsubstituted system showed a strong initial growth followed, after only 2 h, by a marked decrease of the production rate. By elaborating hydrogen production data from other reports included in this review, we ascertained that such behavior is actually rather

common for organic sensitizers. An unprecedented detailed stability investigation of the dye under the irradiation conditions of the photocatalytic test (Figure 21c) clearly associated this finding to the strong photodegradation of the dye. Indeed, after 20 h the concentration of dye **34** remained substantially unvaried whereas only 30% of molecules of **25** survived at the end of the experiments. Interestingly, if dye degradation is taken into account and the hydrogen production data normalized to the amount of residual dye during irradiation, the intrinsic performances of the catalyst based on **31** – **35** can now be correlated to the optical properties of the dyes. Long-term photocatalytic studies confirmed that the hydrogen production rate of the catalyst sensitized by **34** remained stable even after 90 h of prolonged irradiation (Figure 21d). This unprecedented result is valuable in view of industrial applications, where molecular activity must be necessarily associated to long-term stability under operational conditions. In summary, the improved overall performance of the **34**-based material is the direct consequence of the improved optical properties originating by the thiophene substitution and by the remarkable stability under irradiation. This favorable feature has been associated to the presence of the alkyl chains on the thiophene ring, as found in the aforementioned examples, by impeding dye aggregation and detrimental intermolecular interactions.

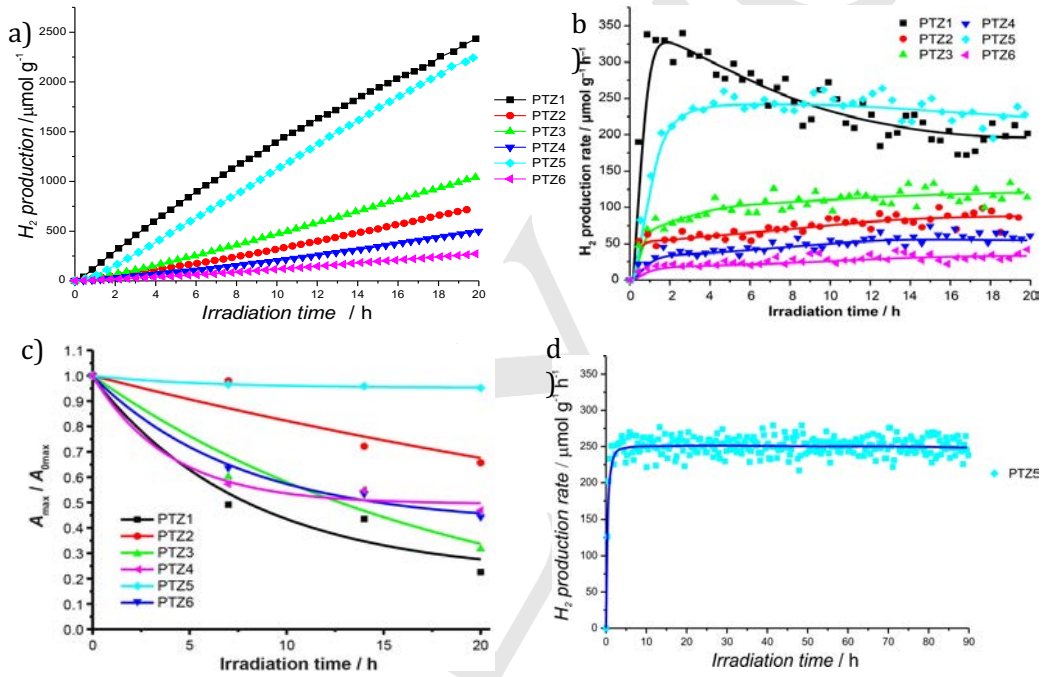

Figure 21: Photocatalytic hydrogen production for dyes **31 – 35**: a) amount of evolved hydrogen vs time; b) rate of hydrogen production; c) degradation studies; d) long-term stability study under irradiation. Reprinted from ref., [60] with permission. Copyright 2015 Wiley-VCH.

A similar effect has been reported for the mono-branched benzo[*b*]phenothiazines **38** – **40**,[62] where the photocatalysts exhibited improved stability and hydrogen production when thiophene spacers were inserted in the D-π-A framework. In particular, the dye with the longest spacer (**40**) showed the best activity, with a TON of 4460 and a AQY of 1.65% at 420 nm. Time-resolved results combined with DFT computations suggested that the spacer can reduce charge recombination and enhance charge injection to TiO_2.

In the study on carbazole dyes **41** and **42** the stronger light harvesting properties of the latter dye, containing a quaterthiophene spacer, with hexyl side chains on each heteroaromatic ring, are effectively translated to higher performances compared to the former dye with no spacer.[30a] However, as the authors correctly pointed out, the very simple dye **41** showed relatively high TON, thus not completely justifying the complicate and expensive synthetic route to the more complex dye. As a matter of fact, **42** could even suffer from some steric hindrance on TiO_2 surface thus hindering the correct protons flow to Pt nanoparticles to produce hydrogen. Diketopyrrolopyrrole dyes **43** and **44** showed interesting efficiencies.[30c] In particular, the replacement of the conventional cyanoacrylic A group of **43** with the dicyanovinyl group in **44** afforded enhanced optical properties and more efficient H_2 evolution (TON of ~ 10 000 in aqueous TEOA solution), despite the weaker linkage to the TiO_2 surface due to the absence of the carboxylic group. The combined presence of the rigid diketopyrrolopyrrole and thiophene rings afforded an improved photostability over 80 h of irradiation. Once again, the beneficial effects of the heteroaromatic moieties in reducing the charge recombination and enhancing charge injection have been demonstrated.

The effect of inserting a thiophene spacer was also evaluated for the coumarin dyes **18** – **22**.[55] In this study the overall water splitting process, with the simultaneous production of H_2 and O_2, has been experimentally followed. The experiments clearly showed that the thiophene-substituted sensitizers **21** and **22** were more stable, thus allowing more efficient water splitting compared to dyes **18** – **20**, where either the spacer was absent or a simple vinylene or mono-thiophene spacer was present (Figure 22).

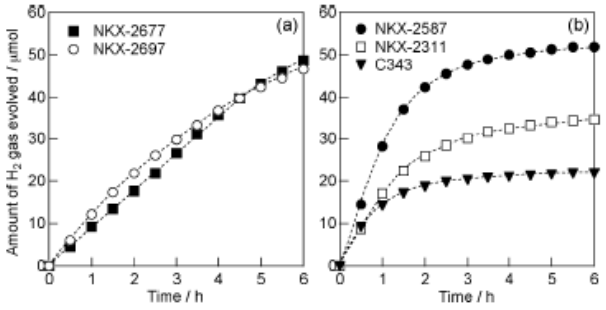

Figure 22: Amount of evolved hydrogen for **18 – 22**. Reproduced from ref. [55] with permission from The Royal Society of Chemistry.

The dye stability was investigated by CV in water, where a reversible current peak in the reverse cathodic scan was present, indicating that the oxidized state is stable enough to be regenerated by the redox couple (Figure 23). The same feature was absent in the CV scans of **18** – **20**. Thus, in those cases the dye oxidized form is less stable, strongly reacting with water or with the evolved oxygen and affording photo-inactive species. Although the absolute efficiency was rather low (STH <0.1% at 500 nm) the oligo-thiophene derivatives demonstrated high durability in water and tolerance to O_2 due to the ability of the thiophene rings to delocalize the positive charge of the radical cation, as confirmed by transient absorption spectroscopy results.

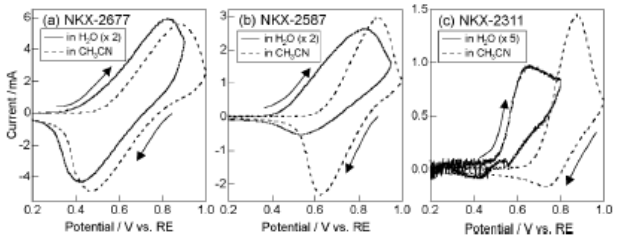

Figure 23: CV curves of coumarin dyes **21** (NKX-2677), **20**, (NKX-2587), and **19** (NKX-2311) adsorbed on a porous TiO_2 electrode in a dehydrated acetonitrile or aqueous 0.1 M of $LiClO_4$ as a supporting electrolyte. Reproduced from ref., [55] with permission from The Royal Society of Chemistry.

Table 2: Summary of dye performances in H_2 production from literature.

Name	λ_{max} (nm)	ε 10^3 ($M^{-1}cm^{-1}$)	solvent	HOMO[a,b] (eV)	LUMO[a,c] (eV)	Dye Loading (µmol/100 mg of Pt-TiO_2)	TON	SED	pH	Ref.
Thionine	600	-	H_2O	-	-	17.6	318 (20 h)[d]	TEOA	7	[40]
Methylene Blue	665	-	H_2O	-	-	7.5	320 (20 h)[d]	TEOA	7	[40]
Nile blue A	640	-	H_2O	-	-	7.9	462 (20 h)[d]	TEOA	7	[40]
Eosin Y	518	-	H_2O	-	-	15.6	1773 (20 h)[d]	TEOA	7	[40]
Rhodamine B	555	-	H_2O	-	-	11.1	1117 (20 h)[d]	TEOA	7	[40]
Safranine O	519	-	H_2O	-	-	14.8	622 (20 h)[d]	TEOA	7	[40]
Alizarin	520	6.7	TEOA 8%	-	-	0.25	6326 (92 h)	TEOA	9	[41]
Alizarin Red	550	5.5	TEOA 8%	-	-	0.25	6342 (80 h)	TEOA	9	[41]
Eosin Y	-	-	TEOA 8%	-	-	0.25	104 (2 h)	TEOA	9	[41]
Coumarin 343	-	-	TEOA 8%	-	-	0.25	127 (2 h)	TEOA	9	[41]
1 (D-H)	433	27.4	THF	-5.29	-2.81	1	270 (5 h)[e]	EDTA	3	[30b]
2 (DMOM)	432	26.7	THF	-5.27	-2.81	1	570 (5 h)[e]	EDTA	3	[30b]
3	433	31.6	THF	-5.27	-2.82	1	730 (5 h)[e]	EDTA	3	[30b]
4	433	27.6	THF	-5.26	-2.78	1	800 (5 h)[e]	EDTA	3	[30b]
5	432	35.5	THF	-5.28	-2.80	1	530 (5 h)[e]	EDTA	3	[30b]

1 (HD)	433	27.4	THF	-5.57	-3.16	10	8 (4 h)	EDTA	3	[48]
6	442	27.4	THF	-5.69	-3.21	10	5.4 (4 h)	EDTA	3	[48]
2 (MOD)	432	26.4	THF	-5.70	-3.25	10	17 (4 h)	EDTA	3	[48]
7	456	29.8	THF	-5.71	-3.44	10	15 (4 h)	EDTA	3	[48]
8	433	37.1	CH_3OH	-5.42	-2.91	10	954 (6 h)	TEOA	7	[30e]
9	482	31.9	CH_3OH	-5.27	-2.99	10	1400 (6 h)	TEOA	7	[30e]
10	497	41.3	CH_3OH	-5.22	-3.03	10	1432 (6 h)	TEOA	7	[30e]
11	502	44.8	CH_3OH	-5.28	-3.03	10	1466 (6 h)	TEOA	7	[30e]
12	542	66.8	CH_3OH	-5.12	-3.05	10	1864 (6 h)	TEOA	7	[30e]
13	509	25.0	CH_2Cl_2	-5.52	-3.42	-[f]	30 µmol (10 h)[g]	CH_3OH	-[c]	[51]
14	533	20.2	CH_2Cl_2	-5.57	-3.60	-[f]	~13 µmol (10 h)[g]	CH_3OH	-[c]	[51]
15	440	35.3	DMF:EtOH 1:1	-5.59	-3.04	-[f]	60 µmol (90 min)[g]	TEOA	10	[54]
16	460	44.3	DMF:EtOH 1:1	-5.75	3.57	-[f]	98 µmol (90 min)[g]	TEOA	10	[54]
17	470	70.7	DMF:EtOH 1:1	-5.72	-3.51	-[f]	111 µmol (90 min)[g]	TEOA	10	[54]
23	476	13.2	GBL[h]	-5.40	-3.21	3	380 (5 h)	TEOA	7	[59]
24	467	13.4	GBL[h]	-5.42	-3.21	3	440 (5 h)	TEOA	7	[59]
25	466	13.3	GBL[h]	-5.43	-3.20	3	606 (5 h)	TEOA	7	[59]
26	464	13.6	GBL[h]	-5.43	-3.20	3	800 (5 h)	TEOA	7	[59]
27	463	13.5	GBL[h]	-5.43	-3.20	3	1026 (5 h)	TEOA	7	[59]
28	433	14.0	CH_3OH	-5.97	-3.12	15	860 (10 h)	TEOA	7	[30d]
29	425	16.0	CH_3OH	-5.96	-3.05	15	1250 (10 h)	TEOA	7	[30d]
30	455	16.8	CH_3OH	-6.15	-3.43	15	1397 (10 h)	TEOA	7	[30d]
25 (PTZ1)	460	13.6	THF	-5.62	-3.52	5.94	82 (20 h)	TEOA	7	[60]
31	471	34.0	THF	-5.38	-3.33	5.96	24 (20 h)	TEOA	7	[60]
32	470	57.8	THF	-5.49	-3.25	6.02	35 (20 h)	TEOA	7	[60]
33	477	56.2	THF	-5.50	-3.17	5.98	17 (20 h)	TEOA	7	[60]
34	478	35.4	THF	-5.39	-3.08	5.96	75 (20 h)	TEOA	7	[60]
35	490	39.2	THF	-5.45	-3.07	5.96	9 (20 h)	TEOA	7	[60]
36	471	32.0	THF	-5.50	-3.70	3.0 (0.1)	59 (678) (20 h)	TEOA	7	[61]
37	470	28.0	THF	-5.50	-3.70	3.0 (0.1)	29 (396) (20 h)	TEOA	7	[61]
38	388	5.1	THF	-5.76	-3.42	1.95[i]	483 (16 h)	TEOA	7	[62]
39	446	20.3	THF	-5.67	-3.45	2.75[i]	3510 (16 h)	TEOA	7	[62]
40	451	22.2	THF	-5.45	-3.46	2.90[i]	4460 (16 h)	TEOA	7	[62]
41	409	42.7	$CHCl_3$	-6.45	-3.42	1[j]	6751 (6 h)	TEOA	7	[30a]
42	510	40.2	$CHCl_3$	-5.05	-2.98	1[j]	9051 (6 h)	TEOA	7	[30a]
43	650	58.2	CH_2Cl_2	-5.39	-3.62	2.5	6720 (10 h)	TEOA	7	[30c]

44	674	108.2	CH_2Cl_2	-5.40	-3.75	2.5	9664 (10 h)	TEOA	7	[30c]

[a]HOMO and LUMO energies have been referred to vacuum using a value of - 4.5 eV vs vacuum for NHE (Ref. 45a). [b]To be compared with a value of -0.5 V vs NHE (– 4.0 eV vs vacuum) for the CB of TiO_2. [c]To be compared with the oxidation potentials of the SEDs: TEOA = +0.97 vs NHE (HOMO = -5.5 eV vs vacuum); EDTA = -0.01 V vs NHE (HOMO = -4.4 eV vs vacuum) (Ref. 54).[] [d]Photocatalytic tests have been done on TiO_2 without Pt. [e]TON values have been estimated by us from the graphs reported in the article. [f]No reference to pH or to dye loading in the text. [g]There is no reference to the amount of photocatalyst or dye loading in the text; TON calculation is thus not possible; moles of evolved hydrogen have been reported for comparison. [h]GBL = γ-butyrolactone. [i]Dye loading has been calculated through absorption spectra difference prior and after dye loading. [j]Nafion coated TiO_2/Pt nanoparticles have been used for hydrogen tests.

Conclusions

We have reviewed the use of metal-free organic sensitizers in the photocatalytic hydrogen production and water splitting. The studies demonstrated that the molecular design is critical to determine the relevant molecular properties for an efficient photocatalytic activity and required stability over long periods of time under conditions (prolonged irradiation, presence of water and/or oxygen) where aromatic dyes are typically fragile. The donor-acceptor D-π-A architecture is found to be the most versatile and of general applicability. A variety of D, A, and π molecular fragments with different chemical, optical, energetic, and stability properties can be included for efficient molecular design and attention to the synthetic access, allowing a virtually infinite number of structural combinations. Using suitable donor cores, both mono- and di-branched geometries can be applied, further extending the diversity of the molecular design.

Relatively few, though representative, donor moieties have been investigated. Amongst the others, the TAA and PTZ cores are the most investigated scaffolds thanks to their chemical structure and presence of proper functionalization sites for the insertion of required properties. In particular, the introduction of hydrophobic or hydrophilic side groups allowed a careful design optimization for detailed comparative studies and enhanced performances in the photocatalytic tests.

The introduction of thiophene-based spacers in the π framework resulted highly beneficial in terms of enhanced light harvesting and long-term stability under irradiation. The chemical nature of the heteroaromatic ring provides a large versatility (mono- and oligo-thiophene as well as fused polycyclic units) for molecular design. Furthermore, relatively easy and up-scalable synthetic routes are available. By using a proper combination of heterocyclic units and exploiting ring substitution by side polar and apolar groups, optical and energetic properties can be finely tuned. Furthermore, the presence of the thiophene rings, in combination with appropriate ring substituents, provides enhanced stability under light soaking suppressing detrimental intermolecular phenomena and stabilizing the oxidized form of the dye following electron injection to the n-type semiconductor.

Despite these encouraging results, the absolute efficiencies are still unsatisfactory, both in terms of STH and TON, typically lower than 1% and 1 x 10^4, respectively. However, stable hydrogen generation rates over long periods have been demonstrated, thus successfully addressing one of the most critical issues of organic components in solar devices.

In comparison with the vast literature on DSSC and other molecular–based materials science fields, with which the matter here reviewed shares many aspects, the study of organic sensitizers for artificial photosynthesis is still in its infancy. Although the donor-acceptor architecture, both in the mono- and multi-branched geometry, has been demonstrated aa a very versatile approach allowing to obtain encouraging efficiencies, the number of applied donor, spacer and acceptor units is still relatively limited in comparison with the abundance of scaffolds available in organic chemistry and already exploited in other materials science sectors, from photovoltaics to transistors and nonlinear optics.

Therefore, a first progress scheme resides in the design of novel donor-acceptor sensitizers with a larger variety of constituting sub-units, with more sophisticated and tailored properties for enhanced photocatalytic efficiency and stability (higher TON and TOF values). However, the future work cannot be limited to these aspects. The dye-sensitized solar production of fuels and chemicals (i.e., hydrogen as well as other fuels and chemicals originating from water and CO_2) necessarily requires an integrated approach covering photocatalytic and PEC devices. Dye-sensitized PEC (DS-PEC) was not the object of the present review. However, we stress the fact that, compared to dye-sensitized photocatalytic hydrogen production, DS-PEC have been even more rarely investigated.[70] The majority of reports refers to the use of molecular sensitizers for active photoanodes (oxidation of water to oxygen)[71] and, more rarely, to active photocathodes (reduction of water to hydrogen).[31c,72] The investigation on tandem devices, with both active photoanodes and photocathodes, is limited to only very few preliminary examples.[73]

In this context the design of molecular sensitizers is still largely dominated by organometallic systems, often referred to common and simple complexes (e.g. Ru complexes with bipyiridine-based ligands). The use of metal-free organic dyes in DS-PEC is basically still absent in the scientific literature, with some rare exceptions for photoanodes,[74] photocathodes,[75] and tandem configurations.[76] In particular, the work by L. Sun and co-workers[76a] is the only present example of organic dye-sensitized tandem DS-PEC so far reported.

It is therefore manifest that a great effort for the design of new generations of organic dyes both for the half-reactions of hydrogen and oxygen photosynthesis and for the entire water splitting process in DS-PEC is needed. In particular, a new concept of integrated molecular sensitizer-catalyst systems is urgently required in order to achieve important efficiencies and promote the study of molecular artificial photosynthesis from the academic to the industrial and commercial phase. This goal requires the use of new donor-acceptor architectures with proper functionalization for conjugation with molecular and non-molecular catalytic centers, both for the reduction and the oxidation of water. By doing this, sustainable approaches must

be kept in mind, including the use of abundant, cheap, and non-toxic starting materials and green synthetic procedures (absence of toxic and volatile solvents).

The ultimate goal, albeit a long term one, is the fabrication of efficient artificial photosynthetic prototypes largely based on abundant and low cost organic components. The achievement of this goal will allow fast industrialization of clean and eco-friendly solar devices competitive with the current methods of production of fuels from fossil sources.

Acknowledgements

AA, BC, and NM thank the Ministero dell'Università e della Ricerca (MIUR-PRIN 2010-11,Grant . 20104XET32) for financial support. T.M. and P.F. thank the Ministero dell'Università e della Ricerca (MIUR-PRIN 2010-11, Grant 2010N3T9M4), EU COST Action CM 1104 and the University of Trieste (project FRA2015) for financial support.

Keywords: dyes • sensitizer • renewable energy • hydrogen • donor-acceptor

[1] a) N. Armaroli, V. Balzani, *Angew. Chem. Int. Ed.* **2007**, *46*, 52-66; b) N. Armaroli, V. Balzani, In *Energy for a Sustainable World*, Wiley-VCH, Weinheim, Germany, **2010**.

[2] a) *Organic, Inorganic and Hybrid Solar Cells: Principles and Practice*, Wiley-IEEE Press, **2012**; b) *Organic and Hybrid Solar Cells* (Eds.: H. Huang, J. Huang), Springer, **2014**; c) *Organic Photovoltaics: Materials, Device Physics, and Manufacturing Technologies* (Eds.: C. Brabec, U. Scherf, V. Dyakonov Wiley-VCH, Weinheim, Germany, **2011**.

[3] a) A. L. Donne, A. Scaccabarozzi, S. Tombolato, S. Binetti, M. Acciarri, A. Abbotto, *Rev. Adv. Sci. Engin.* **2013**, *2*, 170-178; b) M. A. Green, K. Emery, Y. Hishikawa, W. Warta, E. D. Dunlop, *Progr. Photovolt: Res. Appl.* **2015**, *23*, 1-9; c) J. Yan, B. R. Saunders, *RSC Advances* **2014**, *4*, 43286-43314.

[4] Key World Energy Statistics 2015, International Energy Agency (http://www.iea.gov).

[5] N. Armaroli, V. Balzani, *Energy Environ. Sci.* **2011**, *4*, 3193-3222.

[6] N. Armaroli, V. Balzani, *ChemSusChem* **2011**, *4*, 21-36.

[7] G. Centi, S. Perathoner In *Green Carbon Dioxide*, John Wiley & Sons, Inc., **2014**, pp. 1-24.

[8] V. Balzani, A. Credi, M. Venturi, *ChemSusChem* **2008**, *1*, 26-58.

[9] A. Kudo, Y. Miseki, *Chem. Soc. Rev.* **2009**, *38*, 253-278.

[10] a) N. Armaroli, V. Balzani, *Chem. Eur. J.* **2016**, *22*, 32-57; b) *Photoelectrochemical Solar Fuel Production. From Basic Principles to Advanced Devices* (Eds.: S. Gimenéz, J. Bisquert) Springer, **2016**.

[11] M. Cargnello, A. Gasparotto, V. Gombac, T. Montini, D. Barreca, P. Fornasiero, *Eur. J. Inorg. Chem.* **2011**, *2011*, 4309-4323.

[12] A. Fujishima, K. Honda, *Nature* **1972**, *238*, 37-38.

[13] D. E. Scaife, *Solar Energy* **1980**, *25*, 41-54.

[14] a) O. Carp, C. L. Huisman, A. Reller, *Prog. Solid State Chem.* **2004**, *32*, 33-177; b) C. Di Valentin, G. Pacchioni, *Catal. Today* **2013**, *206*, 12-18.

[15] a) L. Amidani, A. Naldoni, M. Malvestuto, M. Marelli, P. Glatzel, V. Dal Santo, F. Boscherini, *Angew. Chem. Int. Ed.* **2015**, *54*, 5413-5416; b) S. K. Cushing, J. Li, F. Meng, T. R. Senty, S. Suri, M. Zhi, M. Li, A. D. Bristow, N. Wu, *J. Am. Chem. Soc.* **2012**, *134*, 15033-15041; c) Z. Liu, W. Hou, P. Pavaskar, M. Aykol, S. B. Cronin, *Nano Lett.* **2011**, *11*, 1111-1116; d) J. Sa, G. Tagliabue, P. Friedli, J. Szlachetko, M. H. Rittmann-Frank, F. G. Santomauro, C. J. Milne, H. Sigg, *Energy Environ. Sci.* **2013**, *6*, 3584-3588.

[16] a) X. Chen, L. Liu, P. Y. Yu, S. S. Mao, *Sci* **2011**, *331*, 746-750; b) A. Gallo , T. Montini, M. Marelli, A. Minguzzi, V. Gombac, R. Psaro, P. Fornasiero, V. Dal Santo, *ChemSusChem* **2012**, *5*, 1800-1811.

[17] a) M. Cargnello, T. R. Gordon, C. B. Murray, *Chem. Rev.* **2014**, *114*, 9319-9345; b) T. R. Gordon, M. Cargnello, T. Paik, F. Mangolini, R. T. Weber, P. Fornasiero, C. B. Murray, *J. Am. Chem. Soc.* **2012**, *134*, 6751-6761.

[18] M. Cargnello, M. Grzelczak, B. Rodríguez-González, Z. Syrgiannis, K. Bakhmutsky, V. La Parola, L. M. Liz-Marzán, R. J. Gorte, M. Prato, P. Fornasiero, *J. Am. Chem. Soc.* **2012**, *134*, 11760-11766.

[19] M. Melchionna, A. Beltram, T. Montini, M. Monai, L. Nasi, P. Fornasiero, M. Prato, *Chem. Commun.* **2016**, *52*, 764-767.

[20] a) Q. Li, B. Guo, J. Yu, J. Ran, B. Zhang, H. Yan, J. R. Gong, *J. Am. Chem. Soc.* **2011**, *133*, 10878-10884; b) Q. Xiang, J. Yu, M. Jaroniec, *Nanoscale* **2011**, *3*, 3670-3678.

[21] a) L. Ferrighi, G. Fazio, C. D. Valentin, *Adv. Mater. Interf.* **2016**, *3*, DOI: 10.1002/admi.201500624; b) H. Zhang, X. Lv, Y. Li, Y. Wang, J. Li, *ACS Nano* **2010**, *4*, 380-386.

[22] a) A. Hagfeldt, G. Boschloo, L. Sun, L. Kloo, H. Pettersson, *Chem. Rev.* **2010**, *110*, 6595-6663; b) B. E. Hardin, H. J. Snaith, M. D. McGehee, *Nature Photonics* **2012**, *6*, 162-169.

[23] M. Liang, J. Chen, *Chem. Soc. Rev.* **2013**, *42*, 3453-3488.

[24] B. O'Regan, M. Gratzel, *Nature* **1991**, *353*, 737-740.

[25] a) X. Fu, J. Long, X. Wang, D. Y. C. Leung, Z. Ding, L. Wu, Z. Zhang, Z. Li, X. Fu, *Int. J. Hydr. En.* **2008**, *33*, 6484-6491; b) J.-J. Zou, C.-J. Liu, K.-L. Yu, D.-G. Cheng, Y.-P. Zhang, F. He, H.-Y. Du, L. Cui, *Chem. Phys. Lett.* **2004**, *400*, 520-523.

[26] J. M. Herrmann, J. Disdier, P. Pichat, *J. Phys. Chem.* **1986**, *90*, 6028-6034.

[27] X. Chen, S. Shen, L. Guo, S. S. Mao, *Chem. Rev.* **2010**, *110*, 6503-6570.

[28] X. Li, J. Yu, J. Low, Y. Fang, J. Xiao, X. Chen, *J. Mater. Chem. A* **2015**, *3*, 2485-2534.

[29] J. Barber, *Chem. Soc. Rev.* **2009**, *38*, 185-196.

[30] a) A. Kumari, I. Mondal, U. Pal, *New J. Chem.* **2015**, *39*, 713-720; b) S. H. Lee, Y. Park, K. R. Wee, H. J. Son, D. W. Cho, C. Pac, W. Choi, S. O. Kang, *Org. Lett.* **2010**, *12*, 460-463; c) K. Narayanaswamy, A. Tiwari, I. Mondal, U. Pal, S. Niveditha, K. Bhanuprakash, S. P. Singh, *Phys. Chem. Chem. Phys.* **2015**, *17*, 13710-13718; d) A. Tiwari, I. Mondal, U. Pal, *RSC Adv.* **2015**, *5*, 31415-31421; e) A. Tiwari, U. Pal, *Int. J. Hydr. En.* **2015**, *40*, 9069-9079.

[31] a) E. Bae, W. Choi, J. Park, H. S. Shin, S. B. Kim, J. S. Lee, *J. Phys. Chem. B* **2004**, *108*, 14093-14101; b) K. Shankar, J. Bandara, M. Paulose, H. Wietasch, O. K. Varghese, G. K. Mor, T. J. LaTempa, M. Thelakkat, C. A. Grimes, *Nano Lett.* **2008**, *8*, 1654-1659; c) W. J. Youngblood, S.-H. A. Lee, K. Maeda, T. E. Mallouk, *Acc. Chem. Res.* **2009**, *42*, 1966-1973.

[32] *Solar Cells - Dye-Sensitized Devices* (Ed.: L. A. Kosyachenko) InTech, **2011**.

[33] a) M. K. Nazeeruddin, C. Klein, P. Liska, M. Grätzel, *Coord. Chem. Rev.* **2005**, *249*, 1460-1467; b) J.-F. Yin, M. Velayudham, D. Bhattacharya, H.-C. Lin, K.-L. Lu, *Coord. Chem. Rev.* **2012**, *256*, 3008-3035.

[34] M. K. Nazeeruddin, F. De Angelis, S. Fantacci, A. Selloni, G. Viscardi, P. Liska, S. Ito, B. Takeru, M. Grätzel, *J. Am. Chem. Soc.* **2005**, *127*, 16835-16847.

[35] A. Abbotto, N. Manfredi, *Dalton Trans.* **2011**, *40*, 12421-12438.

[36] a) Y. Ooyama, Y. Harima, *Eur. J. Org. Chem.* **2009**, *2009*, 2903-2934; b) Y. Ooyama, Y. Harima, *ChemPhysChem* **2012**, *13*, 4032-4080.

[37] a) K. Kakiage, Y. Aoyama, T. Yano, T. Otsuka, T. Kyomen, M. Unno, M. Hanaya, *Chem. Commun.* **2014**, *50*, 6379-6381; b) K. Kakiage, Y. Aoyama, T. Yano, K. Oya, J.-I. Fujisawa, M. Hanaya, *Chem. Commun.* **2015**, *51*, 15894-15897; c) Z. Yao, M. Zhang, H. Wu, L. Yang, R. Li, P. Wang, *J. Am. Chem. Soc.* **2015**, *137*, 3799-3802.

[38] W. J. Youngblood, S.-H. A. Lee, Y. Kobayashi, E. A. Hernandez-Pagan, P. G. Hoertz, T. A. Moore, A. L. Moore, D. Gust, T. E. Mallouk, *J. Am. Chem. Soc.* **2009**, *131*, 926-927.

[39] a) X. Zhang, L. Yu, C. Zhuang, T. Peng, R. Li, X. Li, *RSC Adv.* **2013**, *3*, 14363-14370; b) X. Zhang, L. Yu, C. Zhuang, T. Peng, R. Li, X. Li, *Acs Catal.* **2014**, *4*, 162-170.

[40] D. Chatterjee, *Catal. Commun.* **2010**, *11*, 336-339.

[41] Q. Li, Y. Che, H. Ji, C. Chen, H. Zhu, W. Ma, J. Zhao, *Phys. Chem. Chem. Phys.* **2014**, *16*, 6550-6554.

[42] a) R. Abe, K. Hara, K. Sayama, K. Domen, H. Arakawa, *J. Photochem. Photobiol. A: Chemistry* **2000**, *137*, 63-69; b) Q. Li, Z. Jin, Z. Peng, Y. Li, S. Li, G. Lu, *J. Phys. Chem. C* **2007**, *111*, 8237-8241; c) Z. Yan, X. Yu, Y. Zhang, H. Jia, Z. Sun, P. Du, *Appl. Catal. B: Environmental* **2014**, *160–161*, 173-178.

[43] a) S. Ahmad, E. Guillen, L. Kavan, M. Gratzel, M. K. Nazeeruddin, *Energy Environ. Sci.* **2013**, *6*, 3439-3466; b) B.-G. Kim, K. Chung, J. Kim, *Chem. Eur. J.* **2013**, *19*, 5220-5230; c) L. Kloo, *Chem. Commun.* **2013**, *49*, 6580-6583; d) A. Mishra, M. K. R. Fischer, P. Bäuerle, *Angew. Chem. Int. Ed.* **2009**, *48*, 2474-2499; e) Y. Wu, W. Zhu, *Chem. Soc. Rev.* **2013**, *42*, 2039-2058.

[44] F. Fabregat-Santiago, G. Garcia-Belmonte, I. Mora-Sero, J. Bisquert, *Phys. Chem. Chem. Phys.* **2011**, *13*, 9083-9118.

[45] a) A. J. Bard, L.R. Faulkner, *Electrochemical Methods, Fundamentals and Application*, 2nd Ed., Wiley, **2002**; b) D. T. Sawyer, A. Sobkowiak, J. L. Roberts Jr., *Electrochemistry for Chemist*, 2nd Ed., Wiley, **1995.**

[46] J. Tauc, *Mater. Res. Bull.* **1968**, *3*, 37-46.

[47] a) A. Mahmood, *Solar Energy* **2016**, *123*, 127-144; b) Z. Ning, H. Tian, *Chem. Commun.* **2009**, 5483-5495.

[48] W.-S. Han, K.-R. Wee, H.-Y. Kim, C. Pac, Y. Nabetani, D. Yamamoto, T. Shimada, H. Inoue, H. Choi, K. Cho, S. O. Kang, *Chem. Eur. J.* **2012**, *18*, 15368-15381.

[49] a) *New Trends in Cross-Coupling : Theory and Applications* (Ed.: T. J. Colacot), RSC Publishing, Cambridge, **2015**; b) *Metal-Catalyzed Cross-Coupling Reactions*, 2nd Ed. (Eds.: A. de Meijere, F. Diederich), Wiley, **2004**.

[50] S. M. Feldt, E. A. Gibson, E. Gabrielsson, L. Sun, G. Boschloo, A. Hagfeldt, *J. Am. Chem. Soc.* **2010**, *132*, 16714-16724.

[51] X. Li, S. Cui, D. Wang, Y. Zhou, H. Zhou, Y. Hu, J.-g. Liu, Y. Long, W. Wu, J. Hua, H. Tian, *ChemSusChem* **2014**, *7*, 2879-2888.

[52] N. Miyaura, In *Metal-Catalyzed Cross-Coupling Reactions*, Wiley-VCH, Weinheim, **2008**, pp. 41-123.

[53] a) E. Gabrielsson, H. Ellis, S. Feldt, H. Tian, G. Boschloo, A. Hagfeldt, L. Sun, *Adv. Energy Mater.* **2013**, *3*, 1647-1656; b) D. P. Hagberg, X. Jiang, E. Gabrielsson, M. Linder, T. Marinado, T. Brinck, A. Hagfeldt, L. Sun, *J. Mater. Chem.* **2009**, *19*, 7232-7238.

[54] S. K. Choi, H. S. Yang, J. H. Kim, H. Park, *Appl. Catal. B: Environ.* **2012**, *121*, 206-213.

[55] R. Abe, K. Shinmei, K. Hara, B. Ohtani, *Chem. Commun.* **2009**, 3577-3579.

[56] a) M. Cheng, X. Yang, J. Zhao, C. Chen, Q. Tan, F. Zhang, L. Sun, *ChemSusChem* **2013**, *6*, 2322-2329; b) Y. Hua, S. Chang, D. Huang, X. Zhou, X. Zhu, J. Zhao, T. Chen, W.-Y. Wong, W.-K. Wong, *Chem. Mater.* **2013**, *25*, 2146-2153; c) W.-I. Hung, Y.-Y. Liao, C.-Y. Hsu, H.-H. Chou, T.-H. Lee, W.-S. Kao, J. T. Lin, *Chem. Asian J.* **2014**, *9*, 357-366; d) S. H. Kim, H. W. Kim, C. Sakong, J. Namgoong, S. W. Park, M. J. Ko, C. H. Lee, W. I. Lee, J. P. Kim, *Org. Lett.* **2011**, *13*, 5784-5787.

[57] A. Abbotto, N. Manfredi, C. Marinzi, F. De Angelis, E. Mosconi, J. H. Yum, X. X. Zhang, M. K. Nazeeruddin, M. Gratzel, *Energy Environ. Sci.* **2009**, *2*, 1094-1101.

[58] N. Manfredi, B. Cecconi, A. Abbotto, *Eur. J. Org. Chem.* **2014**, 7069-7086.

[59] J. Lee, J. Kwak, K. C. Ko, J. H. Park, J. H. Ko, N. Park, E. Kim, D. H. Ryu, T. K. Ahn, J. Y. Lee, S. U. Son, *Chem. Commun.* **2012**, *48*, 11431-11433.

[60] B. Cecconi, N. Manfredi, R. Ruffo, T. Montini, I. Romero-Ocana, P. Fornasiero, A. Abbotto, *ChemSusChem* **2015**, *8*, 4216-4228.

[61] N. Manfredi, B. Cecconi, V. Calabrese, A. Minotti, F. Peri, R. Ruffo, M. Monai, I. Romero-Ocana, T. Montini, P. Fornasiero, A. Abbotto, *Chem. Commun.* **2016**, *52*, 6977-6980.

[62] M. Watanabe, H. Hagiwara, A. Iribe, Y. Ogata, K. Shiomi, A. Staykov, S. Ida, K. Tanaka, T. Ishihara, *J. Mater. Chem. A* **2014**, *2*, 12952-12961.

[63] a) K. S. V. Gupta, T. Suresh, S. P. Singh, A. Islam, L. Han, M. Chandrasekharam, *Org. Electron.* **2014**, *15*, 266-275; b) S. Pramjit, U. Eiamprasert, P. Surawatanawong, P. Lertturongchai, S. Kiatisevi, *J. Photochem. Photobiol. A: Chemistry* **2015**, *296*, 1-10; c) C.-H. Yang, S.-H. Liao, Y.-K. Sun, Y.-Y. Chuang, T.-L. Wang, Y.-T. Shieh, W.-C. Lin, *J. Phys. Chem. C* **2010**, *114*, 21786-21794; d) E. M. Barea, C. Zafer, B. Gultekin, B. Aydin, S. Koyuncu, S. Icli, F. F. Santiago, J. Bisquert, *J. Phys. Chem. C* **2010**, *114*, 19840-19848.

[64] a) N. Koumura, Z.-S. Wang, S. Mori, M. Miyashita, E. Suzuki, K. Hara, *J. Am. Chem. Soc.* **2006**, *128*, 14256-14257; b) K. Hara, Z.-S. Wang, Y. Cui, A. Furube, N. Koumura, *Energy Environ. Sci.* **2009**, *2*, 1109-1114; c) G. A. Sewvandi, C. Chen, T. Ishii, T. Kusunose, Y. Tanaka, S. Nakanishi, Q. Feng, *J. Phys. Chem. C* **2014**, *118*, 20184-20192.

[65] F. Bella, C. Gerbaldi, C. Barolo, M. Grätzel, *Chem. Soc. Rev.* **2015**, *44*, 3431-3473.

[66] *High performance pigments*, 2nd Ed. (Eds.: E. B. Faulkner, R.J. Schwartz), Wiley-VCH, Weinheim, **2009**.

[67] S. Zhang, X. Yang, Y. Numata, L. Han, *Energy Environ. Sci.* **2013**, *6*, 1443-1464.

[68] Y.-J. Cheng, S.-H. Yang, C.-S. Hsu, *Chem. Rev.* **2009**, *109*, 5868-5923.

[69] a) P. Chen, J. H. Yum, F. D. Angelis, E. Mosconi, S. Fantacci, S.-J. Moon, R. H. Baker, J. Ko, M. K. Nazeeruddin, M. Grätzel, *Nano Lett.* **2009**, *9*, 2487-2492; b) P. Docampo, S. Guldin, T. Leijtens, N. K. Noel, U. Steiner, H. J. Snaith, *Adv. Mater.* **2014**, *26*, 4013-4030.

[70] N. Queyriaux, N. Kaeffer, A. Morozan, M. Chavarot-Kerlidou, V. Artero, *J. Photochem. Photobiol. C: Photochem. Rev.* **2015**, *25*, 90-105.

[71] a) M. Yamamoto, L. Wang, F. Li, T. Fukushima, K. Tanaka, L. Sun, H. Imahori, *Chem. Sci.* **2016**, *7*, 1430-1439; b) L. Zhang, Y. Gao, X. Ding, Z. Yu, L. Sun, *ChemSusChem* **2014**, *7*, 2801-2804; c) Y. Gao, L. Zhang, X. Ding, L. Sun, *Phys. Chem. Chem. Phys.* **2014**, *16*, 12008-12013; d) Y. Gao, L. Duan, Z. Yu, X. Ding, L. Sun, *Faraday Discuss.* **2014**, *176*, 225-232; e) X. Ding, Y. Gao, L. Zhang, Z. Yu, J. Liu, L. Sun, *ACS Catal.* **2014**, *4*, 2347-2350; f) J. R. Swierk, T. E. Mallouk, *Chem. Soc. Rev.* **2013**, *42*, 2357-2387; g) Y. Gao, X. Ding, J. Liu, L. Wang, Z. Lu, L. Li, L. Sun, *J. Am. Chem. Soc.* **2013**, *135*, 4219-4222.

[72] H. Tian, *ChemSusChem* **2015**, *8*, 3746-3759.

[73] a) Z. Yu, F. Li, L. Sun, *Energy Environ. Sci.* **2015**, *8*, 760-775; b) K. Fan, F. Li, L. Wang, Q. Daniel, E. Gabrielsson, L. Sun, *Phys. Chem. Chem. Phys.* **2014**, *16*, 25234-25240; c) S. Hu, C. Xiang, S. Haussener, A. D. Berger, N. S. Lewis, *Energy Environ. Sci.* **2013**, *6*, 2984-2993; d) L. Alibabaei, H. Luo, R. L. House, P. G. Hoertz, R. Lopez, T. J. Meyer, *J. Mater. Chem. A* **2013**, *1*, 4133-4145.

[74] a) K.-R. Wee, B. D. Sherman, M. K. Brennaman, M. V. Sheridan, A. Nayak, L. Alibabaei, T. J. Meyer, *J. Mater. Chem. A* **2016**, *4*, 2969-2975; b) R. J. Lindquist, B. T. Phelan, A. Reynal, E. A. Margulies, L. E. Shoer, J. R. Durrant, M. R. Wasielewski, *J. Mater. Chem. A* **2016**, *4*, 2880-2893; c) J. R. Swierk, D. D. Méndez-Hernández, N. S. McCool, P. Liddell, Y. Terazono, I. Pahk, J. J. Tomlin, N. V. Oster, T. A. Moore, A. L. Moore, D. Gust, T. E. Mallouk, *Proceed. Nat. Acad. Sci.* **2015**, *112*, 1681-1686.

[75] a) J. Massin, M. Bräutigam, N. Kaeffer, N. Queyriaux, M. J. Field, F. H. Schacher, J. Popp, M. Chavarot-Kerlidou, B. Dietzek, V. Artero, *Interface Focus* **2015**, *5; b)* L. Li, L. Duan, F. Wen, C. Li, M. Wang, A. Hagfeldt, L. Sun, *Chem. Commun.* **2012**, *48*, 988-990; c) J. M. Gardner, M. Beyler, M. Karnahl, S. Tschierlei, S. Ott, L. Hammarström, *J. Am. Chem. Soc.* **2012**, *134*, 19322-19325.

[76] a) F. Li, K. Fan, B. Xu, E. Gabrielsson, Q. Daniel, L. Li, L. Sun, *J. Am. Chem. Soc.* **2015**, *137*, 9153-9159; b) L. Tong, A. Iwase, A. Nattestad, U. Bach, M. Weidelener, G. Gotz, A. Mishra, P. Bauerle, R. Amal, G. G. Wallace, A. J. Mozer, *Energy Environ. Sci.* **2012**, *5*, 9472-9475.

Entry for the Table of Contents (Please choose one layout)

Layout 1:

MICROREVIEW

Text for Table of Contents

Metal-free organic sensitizers for the photocatalytic production of hydrogen and water splitting are reviewed. Studies have outlined the relevance of the molecular design in determining molecular properties and, eventually, photocatalytic efficiencies in terms of evolved gas and stability.

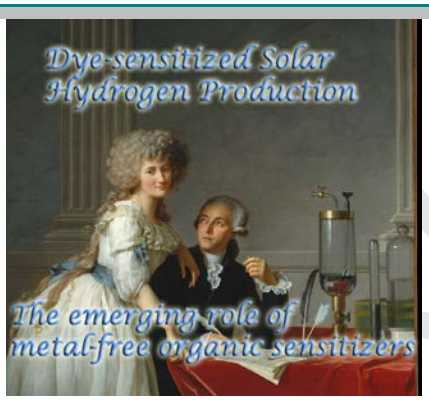

Key Topic: artificial photosynthesis, organic sensitizers

*Bianca Cecconi, Norberto Manfredi, Tiziano Montini, Paolo Fornasiero, and Alessandro Abbotto**

Page No. – Page No.

Dye-Sensitized Solar Hydrogen Production: the Emerging Role of Metal-Free Organic Sensitizers